Molecular Biology of the Cell
Vol. 16, 5356–5372, November 2005

Functions of Adaptor Protein (AP)-3 and AP-1 in Tyrosinase Sorting from Endosomes to Melanosomes[D]

Alexander C. Theos,*† Danièle Tenza,‡ José A. Martina,§ Ilse Hurbain,‡ Andrew A. Peden,‖ Elena V. Sviderskaya,¶ Abigail Stewart,* Margaret S. Robinson,* Dorothy C. Bennett,¶ Daniel F. Cutler,# Juan S. Bonifacino,§ Michael S. Marks,† and Graça Raposo‡

*Cambridge Institute for Medical Research, University of Cambridge, Wellcome Trust, Cambridge CB2 2XY, United Kingdom; †Department of Pathology and Laboratory Medicine, University of Pennsylvania, Philadelphia, PA 19104; ‡Institut Curie, Centre National de la Recherche Scientifique-Unité Mixte de Recherche 144, Paris 75248, France; §Cell Biology and Metabolism Branch, National Institute of Child Health and Human Development, National Institutes of Health, Bethesda, MD 20892; ‖Genentech, South San Francisco, CA 94080; ¶Department of Basic Medical Sciences, St. George's Hospital Medical School, London SW17 ORE, United Kingdom; and #MRC Laboratory for Molecular Cell Biology, Cell Biology Unit, and Department of Biochemistry and Molecular Biology, University College London, London WC1E BT, United Kingdom

Submitted July 13, 2005; Revised August 29, 2005; Accepted September 1, 2005
Monitoring Editor: Sandra Schmid

Specialized cells exploit adaptor protein complexes for unique post-Golgi sorting events, providing a unique model system to specify adaptor function. Here, we show that AP-3 and AP-1 function independently in sorting of the melanocyte-specific protein tyrosinase from endosomes to the melanosome, a specialized lysosome-related organelle distinguishable from lysosomes. AP-3 and AP-1 localize in melanocytes primarily to clathrin-coated buds on tubular early endosomes near melanosomes. Both adaptors recognize the tyrosinase dileucine-based melanosome sorting signal, and tyrosinase largely colocalizes with each adaptor on endosomes. In AP-3-deficient melanocytes, tyrosinase accumulates inappropriately in vacuolar and multivesicular endosomes. Nevertheless, a substantial fraction still accumulates on melanosomes, concomitant with increased association with endosomal AP-1. Our data indicate that AP-3 and AP-1 function in partially redundant pathways to transfer tyrosinase from distinct endosomal subdomains to melanosomes and that the AP-3 pathway ensures that tyrosinase averts entrapment on internal membranes of forming multivesicular bodies.

INTRODUCTION

Sorting of integral membrane proteins among post-Golgi organelles is facilitated by cytoplasmic coats, including the ubiquitously expressed, heterotetrameric adaptor protein (AP) complexes. By binding cytoplasmic sorting signals on cargo proteins, AP complexes recruit cargo to patches on donor membranes that bud to form vesicles or tubules destined to fuse with target membranes (Bonifacino and Traub, 2003; Robinson, 2004). Genetic analyses have shown that whereas deficiency of AP-1 or AP-2 results in embryonic lethality, AP-3 deficiency is not lethal and results in severe phenotypes only in specific tissues (reviewed in Boehm and Bonifacino, 2002). Thus, the transport pathways in which AP-3 functions are likely redundant in most cell types but necessary for unique events in certain cells. Defining these pathways and those involving the essential APs will be necessary to fully understand endosomal maturation and the formation of tissue-specific organelles.

How and where AP-3 functions in "nonspecialized" cells is controversial. Yeast AP-3 binds to cytoplasmic dileucine-like sorting signals of cargo, such as alkaline phosphatase and Vam3p, and facilitates their biosynthetic traffic to the vacuole in a pathway that bypasses the prevacuolar compartment, analogous to the mammalian multivesicular late endosome/multivesicular body (MVB) (reviewed in Burd *et al*., 1998). Mammalian AP-3 also binds preferentially in vitro to dileucine- and tyrosine-based sorting signals of lysosomal transmembrane proteins (Bonifacino and Traub, 2003; Janvier *et al*., 2003), implying a function in lysosomal sorting (Odorizzi *et al*., 1998; Robinson and Bonifacino, 2001). Consistent with this function, a subset of lysosomal membrane proteins in AP-3-deficient fibroblasts undergo increased recycling via the cell surface (reviewed in Starcevic *et al*., 2002). Whereas some evidence may support a role for AP-3 in direct transport from the *trans*-Golgi network (TGN) to lysosomes (Rous *et al*., 2002; Ihrke *et al*., 2004), other data are most consistent with a primary role in sorting from early

This article was published online ahead of print in *MBC in Press* (http://www.molbiolcell.org/cgi/doi/10.1091/mbc.E05–07–0626) on September 14, 2005.

[D] The online version of this article contains supplemental material at *MBC Online* (http://www.molbiolcell.org).

Address correspondence to: Graça Raposo (g.raposo@curie.fr).

Abbreviations used: AP, adaptor protein; IEM, immunoelectron microscopy, ILV, intralumenal vesicle; LRO, lysosome-related organelle; MVB, multivesicular body; PAG, protein A-gold; PB, phosphate buffer; Tf, transferrin.

endosomes. AP-3-containing coats have been localized not only to the TGN (Simpson *et al*., 1997) but also more prominently to endosomal membranes in a number of cell types (Simpson *et al*., 1996; Dell'Angelica *et al*., 1997, 1999; Simpson *et al*., 1997) and in particular to tubulovesicular domains of early endosomes in HepG2 cells; in these cells, AP-3 is thought to divert membrane proteins such as lysosomal-associated membrane protein (LAMP)-1 away from recycling to the cell surface and toward lysosomes (Peden *et al*., 2004). However, loss of AP-3 function does not affect the gross distribution of LAMP-1 and other cargo to their target late endosome/lysosome destination in HepG2 and fibroblast systems. The dispensability of AP-3 function in these cells for late endosome/lysosome localization has made it difficult to dissect the interrelationships among AP-3-dependent and -independent sorting and the pathways in which they participate.

AP-3-deficient animals are characterized by severe defects in organelle function in specific tissues, including dense granules in platelets, lytic granules in cytotoxic T-cells, a subset of synaptic vesicles in some neurons, and melanosomes of pigment cells (Starcevic *et al*., 2002; Stinchcombe *et al*., 2004; Seong *et al*., 2005). These phenotypes imply that AP-3-dependent sorting is uniquely required for the biogenesis of specialized structures, collectively referred to as lysosome-related organelles (LROs) (Dell'Angelica *et al*., 2000; Blott and Griffiths, 2002). LROs thus provide a context in which AP-3 function is best defined. A candidate LRO cargo for AP-3-dependent sorting is tyrosinase, a type I integral membrane protein whose enzymatic activity mediates the limiting step in melanin biosynthesis within melanosomes. A dileucine-based signal within the cytoplasmic domain of tyrosinase binds in vitro to AP-3 (Honing *et al*., 1998) and is required for efficient sorting in nonpigment cells (Blagoveshchenskaya *et al*., 1999; Calvo *et al*., 1999; Simmen *et al*., 1999; Wang *et al*., 1999). Moreover, tyrosinase is mislocalized in melanocytes derived from AP-3-deficient Hermansky-Pudlak Syndrome patients (Huizing *et al*., 2001). Although these data imply a direct role for AP-3 in sorting tyrosinase to melanosomes, several questions remain unanswered. Does AP-3 mediate transport from the TGN or from endosomes? Because AP-3-deficient melanocytes are not totally devoid of mature melanosomes (Nguyen *et al*., 2002), can an alternative AP-dependent pathway direct tyrosinase to the melanosome? A candidate is AP-1, recently implicated in the biogenesis of another LRO, the Weibel-Palade body (Lui-Roberts *et al*., 2005). Finally, given the unique dynamics of the endosomal system in melanocytes (Raposo *et al*., 2001), are AP functions in sorting to melanosomes related to those in nonspecialized cell types? To address these questions, we have quantitatively localized AP-3, AP-1, and tyrosinase within melanocytes and defined how AP-3-deficiency affects tyrosinase transport. The results indicate that tyrosinase traffics through the early endocytic system and that mammalian AP-3 functions on early endosomes to divert tyrosinase away from a pathway leading to multivesicular endosomes and toward one leading to melanosomes. Moreover, they reveal a dynamic interplay between AP-3 and AP-1 in endosomal sorting to provide alternative routes to the melanosome.

MATERIALS AND METHODS

Chemicals and Antibodies

Chemicals and tissue culture reagents were from Sigma-Aldrich (St. Louis, MO) unless otherwise noted. Monoclonal antibodies (mAbs), their targets, and their sources were as follows: TA99 (Mel-5) to Tyrp1 (American Type Culture Collection, Manassas, VA); 100/3 to γ-adaptin and 100/2 to α-adaptin (Sigma-Aldrich), monoclonal antibody to δ-adaptin (Peden *et al*., 2004), anti-clathrin heavy chain (BD Transduction Laboratories, San Diego, CA); and H68.4 to transferrin (Tf) receptor (Zymed Laboratories, South San Francisco, CA). Polyclonal rabbit antisera to δ- μ3-, and β3A-adaptins (Simpson *et al*., 1997); σ3-adaptin (Simpson *et al*., 1996; Dell'Angelica *et al*., 1997, 1999; Simpson *et al*., 1997); Pmel17 (αPEP13h; Berson *et al*., 2001); γ-adaptin (Seaman *et al*., 1996); STO 125 (gift from S. Tooze, Cancer Research UK, London, United Kingdom) (Dittie *et al*., 1996); Hrs (Sachse *et al*., 2002) (gift from S. Urbé, University of Liverpool, Liverpool, United Kingdom); and clathrin light chain (gift from F. Brodsky, Department of Biopharmaceutical Sciences, University of California, San Francisco, San Francisco, CA) (Acton *et al*., 1993) have been described previously. Sheep anti-human TGN46 was from Serotec (Raleigh, NC). Rabbit anti-mouse immunoglobulin (Ig)G was from Dakopatt (Glostrup, Denmark); Alexa488- and Alexa594-conjugated secondary antibodies, Tf-fluorescein isothiocyanate (FITC), and anti-FITC antibodies were from Invitrogen (Carlsbad, CA); Tf-horseradish peroxidase (HRP) was from Pierce Chemical (Rockford, IL); HRP-conjugated anti-mouse and anti-rabbit IgG were from GE Healthcare (Little Chalfont, Buckinghamshire, United Kingdom); and FITC- and Texas Red-conjugated isotype-specific secondary antibodies were from Southern Biotechnology (Birmingham, AL). Protein A conjugated to 10- or 15-nm gold particles was from Cell Microscopy Center (AZU, Utrecht, The Netherlands).

Cells

MNT-1 human melanoma (Raposo *et al*., 2001) and mouse melan-a cells (Bennett *et al*., 1987) were maintained as described previously. MNT-1 cells (5×10^6 per transfection) were transfected by electroporation using the Equibio Optimix kit (Ozyme, St. Quentin Yvelines, France) and a Bio-Rad electroporation unit (Bio-Rad, Hercules, CA) according to the manufacturers' instructions with a single pulse (140 V, 3.25 μF and infinite resistance). Transfected cells were reseeded on coverslips and cultured for 24 or 48 h. Melan-pe cells were obtained by immortalization of primary mouse melanocytes from B6Pin.C3-*Ap3b1*^{pe}/*Ap3b1*^{pe} (pearl) mice (The Jackson Laboratory, Bar Harbor, ME) according to published protocols (Sviderskaya *et al*., 1997) (available at http://www.sghms.ac.uk/depts/anatomy/pages/protocols/msmelpri.html).

Recombinant DNA Constructs, Yeast Three-Hybrid, and Glutathione S-Transferase (GST) Pull-Down Analyses

HRP-tyrosinase chimerae HRP-tyr and HRP-tyrAA (Blagoveshchenskaya *et al*., 1999) and GAL4AD fusions to γ1, αC, δ, and ε-adaptins in pGADT7 (BD Biosciences Clontech, Palo Alto, CA) (Bonifacino and Traub, 2003; Janvier *et al*., 2003) have been described previously. GAL4BD fusion constructs were made by PCR amplification from plasmids encoding mouse tyrosinase (31 C-terminal residues), Tyrp1 (35 C-terminal residues), and Tyrp2 (29 C-terminal residues) and in-frame cloning into the EcoRI-PstI (tyrosinase, Tyrp1) or XmaI-PstI sites (Tyrp2) of pBridge (BD Biosciences Clontech). Mutants of GAL4BD-Tyrosinase were obtained by PCR-directed mutagenesis. The σ AP subunits were amplified by PCR and subcloned into the Not I-BglII sites of pBridge-Tyrosinase, pBridge-Typr1 and pBridge-Tyrp2. GST-Tyrosinase (wild-type; WT) was obtained by in frame cloning of sequence encoding the 31 C-terminal residues of mouse tyrosinase into the EcoRI site of pGEX-5X-1 (GE Healthcare), and the mutants were generated by PCR-directed mutagenesis. Production and purification of GST fusion proteins, GST pull-downs, and yeast three-hybrid assays were performed as described previously (Bonifacino and Traub, 2003; Janvier *et al*., 2003).

Production of Anti-Mouse Tyrosinase Antibody

To prepare GST fusion proteins, a fragment encoding lumenal residues 19–476 of mouse tyrosinase was generated by PCR using pTyrs-J template (gift from H. Yamamoto, Tohoku University, Sendai, Japan) (Yamamoto *et al*., 1987), and subcloned into BamHI/EcoRI-cut pGEX-3X (GE Healthcare) to generate pGST-LD. Fusion protein was expressed in XL-1 Blue cells by induction for 5–7 h at 37°C with 0.1 mM isopropyl β-D-thiogalactoside, and purified from inclusion bodies as described previously (Page and Robinson, 1995). Purified protein (0.5 mg/injection) in phosphate-buffered saline (PBS)/0.2% SDS was injected into rabbits at 2- to 6-wk intervals with Complete Freund's Adjuvant by Murex Biotech (Dartford, Kent, United Kingdom), and serum was collected 10 d after the last injection. Affinity-purified antibodies were prepared using purified GST-LD coupled to beads as described previously (Page and Robinson, 1995) and adsorbed against GST bound to Sepharose beads before use.

Immunofluorescence Microscopy, Immunoprecipitation, and Western Blotting

Cells were fixed in PBS containing 2% formaldehyde for 15–30 min at room temperature (RT) and then labeled with primary and fluorescent secondary antibodies as described previously (Berson *et al*., 2001). Cells were analyzed on a DM IRBE microscope (Leica Microsystems, Wetzlar, Germany) equipped with an Orca digital camera (Hamamatsu, Bridgewater, NJ), and images were

captured and manipulated using Improvision OpenLab software (Lexington, MA) with the volume deconvolution package. Immunoprecipitation from lysates of melan-a cells and immunoblotting were essentially as described previously (Berson *et al*., 2001; Peden *et al*., 2002).

Electron Microscopy

Ultracryomicrotomy, Immunogold Labeling, and Analysis. Cells were fixed with 2% (wt/vol) paraformaldehyde (PFA) or with a mixture of 2% (wt/vol) PFA and 0.2% (wt/vol) glutaraldehyde in 0.1 M phosphate buffer (PB), pH 7.4. Cells were processed for ultracryomicrotomy as described previously (Raposo *et al*., 1997). Ultrathin sections were prepared with an Ultracut fetal calf serum ultracryomicrotome (Leica, Vienna, Austria), and single or double immunogold labeled with antibodies and protein A coupled to 10- or 15-nm gold (PAG10 and PAG15). Sections were observed and photographed under a Philips CM120 electron microscope (FEI, Eindoven, The Netherlands). Digital acquisitions were made with a numeric camera Keen View (Soft Imaging System, Munster, Germany).

Internalization of Tf-FITC. Cells were washed with serum-free medium and starved for 45 min before incubation with Tf-FITC (60 μg/ml) for 45 min at 37°C. After washing with ice-cold medium, cells were fixed and processed for ultracryomicrotomy.

Quantification of Immunogold Labeling. The relative distribution of AP-3 and AP-1 in melan-a cells was evaluated by analyzing directly under the electron microscope randomly selected cell profiles from two distinct grids. In total, 450 and 448 gold particles were counted for AP-3 and AP-1, respectively, and assigned to the compartment over which they were located. The definition of the distinct compartments was based on their morphology and their previous characterization by immunogold labeling with different organelle markers (EEA-1 and Hrs for early endosomes; TGN38 and TGN46 for the TGN; and LAMP-1 for late endosomes/lysosomes) and internalization of endocytic tracers (bovine serum albumin-gold and Tf-FITC). Tubulovesicular membranes that were located at the *trans*-side of the Golgi were considered as TGN. Vacuolar endosomes were defined as electron-lucent vacuoles with no internal membranes or few internal vesicles. MVBs were compartments delimited by a membrane with numerous internal vesicles. Electron-dense compartments with no or few internal membranes were classified as lysosomes. Clearly visible tubulovesicular membrane profiles connected to or in close association with endosomal vacuoles, melanosomes, MVBs, and lysosomes were also defined. Melanosome stages were defined by morphology (Raposo *et al*., 2001). Quantification of tyrosinase distribution in melan-a and melan-pe cells was performed on single immunogold-labeled cryosections by counting the number of gold particles in each of the defined compartments (see above) taken randomly in 50 cell profiles. In total, 1033 and 1100 gold particles were counted in melan-a and melan-pe cells, respectively. Results are presented as a percentage of the total number of gold particles in each compartment and represent a mean and SD of two independent experiments. The labeling densities of tyrosinase was estimated in a series of double-labeling experiments to detect tyrosinase and AP-3 or AP-1 in melan-a and melan-pe cells. The monoclonal anti-AP-3 and anti-AP-1 were used in the first step. AP-3- and AP-1-positive membranes were selected under the electron microscope, and 70 images of AP/tyrosinase positive areas were taken with a charge-coupled device camera. Using Adobe Photoshop, images at an end magnification of 80,000× were overlaid with a 5-mm-spaced line lattice. The number of gold particles present on AP-3–positive/AP-3-negative and AP-1-positive/AP-3-negative regions of the compartments was counted. The number of intersections of the distinct membrane domains with the 5-mm line lattice overlay was also counted to give a measure of membrane length (Griffiths, 1993; Peden *et al*., 2004). The number of gold particles per intersection reflected the labeling density for tyrosinase in the different areas. The percentage of AP-3- or AP-1-positive vesicles and buds labeled for tyrosinase in melan-a and melan-pe cells was determined by counting directly on the electron microscope the total number of AP-3 or AP-1-coated vesicles of cells double immunogold labeled for tyrosinase and AP-3 or AP-1.

Whole-Mount Electron Microscopy (EM). Immunogold labeling of AP-3, AP-1, Clathrin, Hrs, Pmel17 (using αPep13h antibody to the cytoplasmic domain), and Tf receptor on whole-mounted cells was performed as described previously (Stoorvogel *et al*., 1996) on cells grown for 2 d on Formvar-coated gold grids. In brief, after washing with minimal essential medium, 20 mM HEPES, pH 7.4, cells were starved for 45 min in the same medium at 37°C and then incubated for 45 min with 50 μg/ml HRP-Tf. Cells were cooled to 4°C and incubated in 3,3′-diaminobenzidine tetrahydrochloride (DAB)-H_2O_2-containing buffer. Soluble cytosolic proteins were removed by permeabilization with saponin, and cells were then fixed with 3% PFA in 0.1 M phosphate buffer, pH 7.4, for 2 h. Immunogold labeling was performed at RT in the presence of saponin and using cold fish gelatin as blocking buffer. After labeling, cells were fixed with 2% glutaraldehyde, rinsed in water, dehydrated in increasing concentrations of ethanol, and dried in a critical point dry apparatus (BAL-TEC, Balzers, Lichtenstein) before EM analysis.

Conventional Electron Microscopy and DAB Cytochemistry. MNT-1 cells transfected with HRP-tyr and HRP-tyrAA for 24 or 48 h were fixed with 2% PFA/0.5% glutaraldehyde in 0.2 M PB, pH 7.4, for 90 min. After several washes with 50 mM Tris-HCl, pH 7.6, cells were treated for 20 min with 0.03% DAB in the presence of 1 μl/ml H_2O_2 (30 vol). Cells were fixed with 2.5% glutaraldehyde in 0.1 M cacodylate buffer for 90 min, postfixed with 2% OsO_4, dehydrated in ethanol, and embedded in Epon. Ultrathin sections were counterstained with uranyl acetate before observation.

DOPA Histochemistry. DOPA histochemistry was carried out as described previously (Boissy *et al*., 1998). The cells were then washed and incubated in 1% osmium tetroxide with 1.5% potassium ferrocyanide in 0.2 M sodium cacodylate buffer for 1 h at RT and then washed before dehydration and embedding for sectioning (Reynolds, 1963).

RESULTS

AP-3 and AP-1 Localize to Distinct Endosomal Buds on Early Endocytic Clusters near Melanosomes

To localize AP-3 and AP-1 in melanocytes, we used immunoelectron microscopy (IEM) with immunogold labeling on ultrathin cryosections and "whole-mounted" cells. We first assessed AP-3 localization in ultrathin cryosections of MNT-1 melanoma cells, a faithful model system for melanosome biogenesis (Berson *et al*., 2001; Kushimoto *et al*., 2001; Raposo *et al*., 2001; Berson *et al*., 2003) and in mouse melan-a immortalized melanocytes. In both MNT-1 and melan-a cells, the bulk of labeling for AP-3 was associated with tubulovesicular clusters of coated vesicles or buds (Supplemental Figure S1, A and B) similar to those described in nonpigmented cells (Peden *et al*., 2004). Most of these clusters were in proximity to vacuolar endosomes and were also often found closely apposed to stage III and IV (i.e., more mature) melanosomes (Figures 1A and S1, A and B). To evaluate the connection of the AP-3-positive tubulovesicular clusters to endosomes and melanosomes, we used whole-mount immunogold labeling (Stoorvogel *et al*., 1996). MNT-1 cells were allowed to internalize Tf-HRP conjugate for 1 h to fill early sorting and recycling endosomes, and then they were treated with DAB and hydrogen peroxide, permeabilized, and immunogold labeled. Cross-linked early endosomes thus look like electron-dense vacuolar and tubular domains with numerous buds. The endosomal tubules and vacuoles label with antibodies to the cytoplasmic domain of Pmel17 (Figures 1C and S1C), an integral membrane protein that passes through early endosomes en route to stage II premelanosomes (Berson *et al*., 2001; Raposo *et al*., 2001). AP-3 is highly concentrated in many of the buds associated with the endosomal tubules and vacuoles, although the buds themselves lack labeling for Pmel17 (arrows in Figures 1C and S1C). Moreover, in cryosections of MNT-1 cells that had internalized Tf-FITC for 1 h before fixation, buds labeled for AP-3 but not for FITC emerge from endosomal tubules labeled for FITC (Figure 1D). Whole-mount analyses corroborate the proximity to melanosomes of AP-3-coated buds continuous with Hrs-positive endosomal vacuoles (Figure 1B) and also reveal the presence of clathrin on the AP-3-containing buds (Figure 1E; also see Supplemental Figure S1B). Quantitative analysis revealed that 41% of AP-3 vesicles and buds also contain clathrin in agreement with findings in HepG2 cells (Peden *et al*., 2004). The labeling of the associated tubules for Pmel17 and Tf-FITC confirms their endocytic nature, whereas the lack of labeling for Pmel17 and Tf-FITC within the buds indicates that they fail to enrich early endocytic cargo. We conclude that in melanocytes, AP-3 is primarily localized to clathrin-coated buds on tubulovesicular elements adjacent to endosomal vacuoles and melanosomes.

Coated buds devoid of AP-3 labeling are often observed near AP-3-labeled buds on the same tubulovesicular clusters

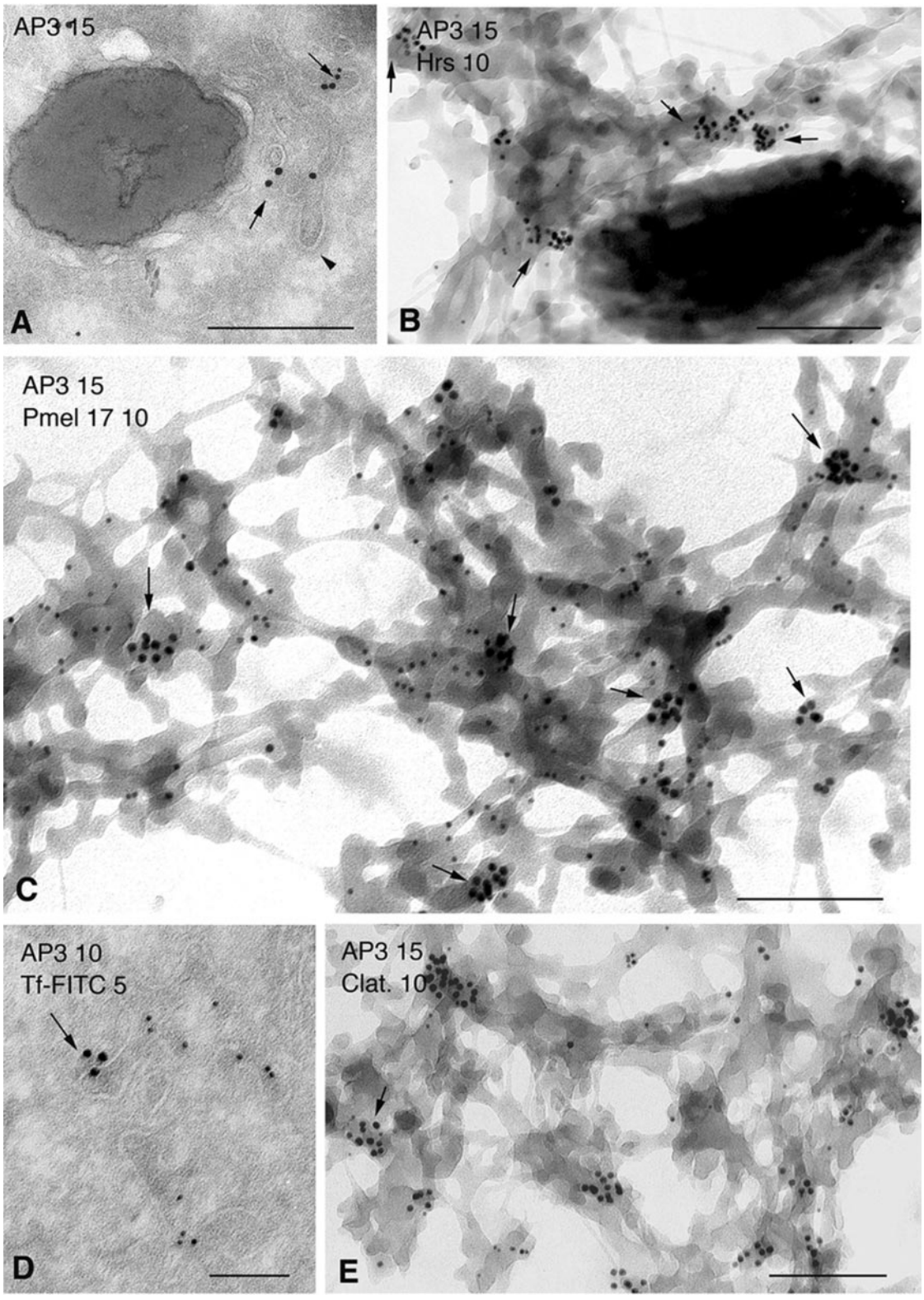

Figure 1. AP-3 localizes to buds near endosomes and melanosomes in MNT-1 cells. (A) Ultrathin cryosections of MNT-1 cells were immunogold labeled for AP-3 (PAG15) or AP-3 (PAG15) and Hrs (PAG10). A region near a stage IV melanosome is shown. Arrows highlight AP-3 labeling in buds and tubules closely apposed to the melanosome. (B, C, and E) MNT-1 cells were incubated at 37°C for 1 h with Tf-HRP and then processed for whole-mount cytochemistry. Cells were immunogold labeled for AP-3 (PAG15) and Hrs (PAG10; B), the cytoplasmic domain of Pmel17 (PAG10; C), or the clathrin light chain (PAG10; E). Arrows point to clusters of AP-3 labeling on endosomal buds closely apposed to melanosomes (B) and linked to electron-dense endosomes that label for Pmel17 (C) and Hrs (B). The AP-3-labeled buds also label for clathrin (E). (D) Ultrathin cryosection of MNT-1 cells incubated at 37°C for 1 h with Tf-FITC and double labeled for AP-3 (PAG10) and FITC (PAG5). Note the continuity of the AP-3 labeled bud to FITC labeled tubules. Bars, 200 nm.

(Figure 1A). Because AP-3 and AP-1 are both present on buds on tubular endosomes in other cell types (Peden *et al*., 2004), we compared their relative distributions in MNT-1 cells. Both AP-3- and AP-1-coated buds are observed on endosomes, as shown by immunogold labeling on budding profiles emanating from DAB-containing tubules by whole-mount EM (Figure 2, A and B) and by double labeling for AP-1 and FITC in cryosections of cells that had previously internalized Tf-FITC (Figure 2, E and F). Like AP-3-coated buds, AP-1-coated buds are often located in the vicinity of Hrs-positive vacuolar endosomes (Figure 2C) and melanosomes (Figure 2, C and D). Although buds and vesicles containing both adaptors are occasionally observed (Figure 2B, inset; ~2% of total labeling for AP-3 and AP-1), labeling for AP-1 and AP-3 was predominantly exclusive, suggesting that the two AP complexes are largely present on distinct endosomal buds (Figure 2, A, B, and D). Quantitative evaluation of the relative distribution of AP-3 and AP-1 in melan-a cells (Table 1) revealed the highest level of labeling for AP-3 in tubulovesicular elements close to endosomal vacuoles (41.5%) and melanosomes (25.8%). In melanocytic cells the highest labeling for AP-1 is also found close to endosomes (39%). Although more enriched than AP-3 in the TGN area and cytoplasmic vesicles, AP-1 is also significantly enriched in tubulovesicular elements close to melanosomes (19%). IFM analysis of MNT-1 cells corroborates with these findings (Supplemental Figure S2). Together, these data indicate that AP-1 and AP-3 most prominently populate distinct buds on endosomal tubules near vacuolar endosomes and melanosomes.

Both AP-3 and AP-1 Bind to the Tyrosinase Sorting Signal

The close apposition of the bulk of AP-3- and AP-1-labeled endosomes to melanosomes suggests that these complexes may sort melanosomal cargo such as tyrosinase and Tyrp1, as suggested previously (Huizing *et al*., 2001; Raposo *et al*., 2001). We therefore tested whether AP-1 and AP-3 directly interact with the tyrosinase and Tyrp1 sorting signals. Post-Golgi sorting of tyrosinase is mediated by a dileucine signal (EERQPLL in mice, EEKQPLL in humans) (Blagoveshchenskaya *et al*., 1999; Calvo *et al*., 1999; Simmen *et al*., 1999) (Figure 3A), which conforms to the D/ExxxLL/I motif recognized by both AP-1 and AP-3 (Bonifacino and Traub, 2003), and Tyrp1 sorting depends on a related sequence (EANQPLL) (Vijayasaradhi *et al*., 1995). Similar signals bind in a yeast three-hybrid assay to the γ1-σ1A and the δ-σ3A or δ-σ3B hemicomplexes of AP-1 and AP-3, respectively (Janvier *et al*., 2003). Using this assay, the tyrosinase cytoplasmic domain interacts with hemicomplexes from AP-1 and AP-3 but not with those of AP-2 and AP-4 (Figure 3B). By contrast, the Tyrp1 cytoplasmic domain binds only weakly to the AP-1 hemicomplex and not at all to AP-3, and the Tyrp2 cytoplasmic domain, which contains only a tyrosine-based motif predicted to bind to AP μ subunits (Figure 3A), did not bind to any hemicomplex (Figure 3B). These data confirm that the tyrosinase cytoplasmic domain binds AP-3 and demonstrate a previously uncharacterized interaction with AP-1.

The interaction of tyrosinase with AP-3 is known to require the conserved, active dileucine-based targeting signal (Honing *et al*., 1998) (Figure 3A). Similarly, the interaction with AP-1 requires the same signal, because mutagenesis of the two conserved leucine residues (L517 and L518) abrogated interactions with both AP-1 and AP-3 hemicomplexes in the three-hybrid assay (Figure 3C). In contrast, mutation of two nonconserved leucine residues (L527 and L528), which are not required for sorting (Simmen *et al*., 1999), had no effect on the interactions (Figure 3C). GST pull-down assays confirmed the interactions of the tyrosinase cytoplasmic domain with the native AP-1 and AP-3 complexes and the dependence of these interactions on leucine residues 517 and 518 but not those at 527 and 528 (Figure 3D). These data confirm that similar sequences are required to direct both sorting of tyrosinase and binding not only to AP-3 but also to AP-1.

Tyrosinase enzyme activity in melanocytes is detected primarily in mature melanosomes (see below; Seiji *et al*., 1963; Yamamoto and Takeuchi, 1981). If localization to melanosomes requires binding to AP-1 and AP-3 in endosomes, then a mutant form lacking the dileucine-based sorting signal should accumulate within the donor endosomal compartments. To test this prediction, we expressed in MNT-1 cells a fusion protein containing HRP in the lumenal domain and the tyrosinase cytoplasmic domain without (HRP-tyr) or with (HRP-tyrAA) a dialanine substitution in the dileucine motif (Blagoveshchenskaya *et al*., 1999). Although not quantitative, the very sensitive peroxidase cytochemical reaction reveals even very low levels of HRP trafficking through an organelle, thus enabling evaluation of the total distribution of the HRP-tyrAA chimera. EM analysis of DAB-treated MNT-1 cells expressing HRP-tyr revealed accumulation of electron-dense DAB reaction product primarily in endosomal tubules and melanosomes, consistent with tyrosinase immunolocalization in mouse melan-a cells (our unpublished data; see below). By contrast, cells expressing HRP-tyrAA accumulate fusion protein primarily in tubular and vacuolar endosomes containing associated buds (Figure 4A) with very little or no accumulation in either the Golgi/TGN area (Figure 4A) or in melanosomes (Figure 4C). HRP-tyrAA also accumulates at the plasma membrane (Figure 4B), as expected for a protein undergoing rapid endocytic recycling. DAB electron-dense deposit was also sometimes observed as clusters in the lumen of compartments that are likely to correspond to MVBs, perhaps reflecting a failure of the mutant protein to be sorted away from a lysosomal destination (Figure 4C). Thus, the distribution of a mutant lacking AP-1 and AP-3 binding sites is consistent with a role for either or both APs in facilitating transport of tyrosinase from endosomes toward melanosomes

Tyrosinase Traffics through Endosomes

To determine whether tyrosinase normally transits through the endocytic pathway, we analyzed quantitatively the steady-state distribution of tyrosinase within melanocytes. Whereas previous analyses have relied on histochemical detection of tyrosinase activity, quantitative analyses require nonenzymatic analyses such as immunogold labeling. Using bacterially expressed GST fusion proteins containing the lumenal domain of mouse tyrosinase, we prepared rabbit polyclonal antisera suitable for IEM analyses of tyrosinase. By immunoblotting, these antisera recognize a specific band of ~70 kDa in whole-cell lysates of melan-a mouse melanocytes but not human melanocytic cells (Supplemental Figure S3A). We therefore used these antisera to analyze tyrosinase localization in mouse melanocytes. Immunofluorescence microscopy and deconvolution analyses of primary mouse melanocytes or melan-a cells with this antibody reveal a vesicular pattern that only partially overlaps with that of other markers of immature (stage II; Pmel17) and mature (stage III and IV; Tyrp1) melanosomes (Supplemental Figure S3B). This partial overlap is consistent with observations using antisera to the tyrosinase cytoplasmic domain (our unpublished data) and may reflect both a steady-state localization

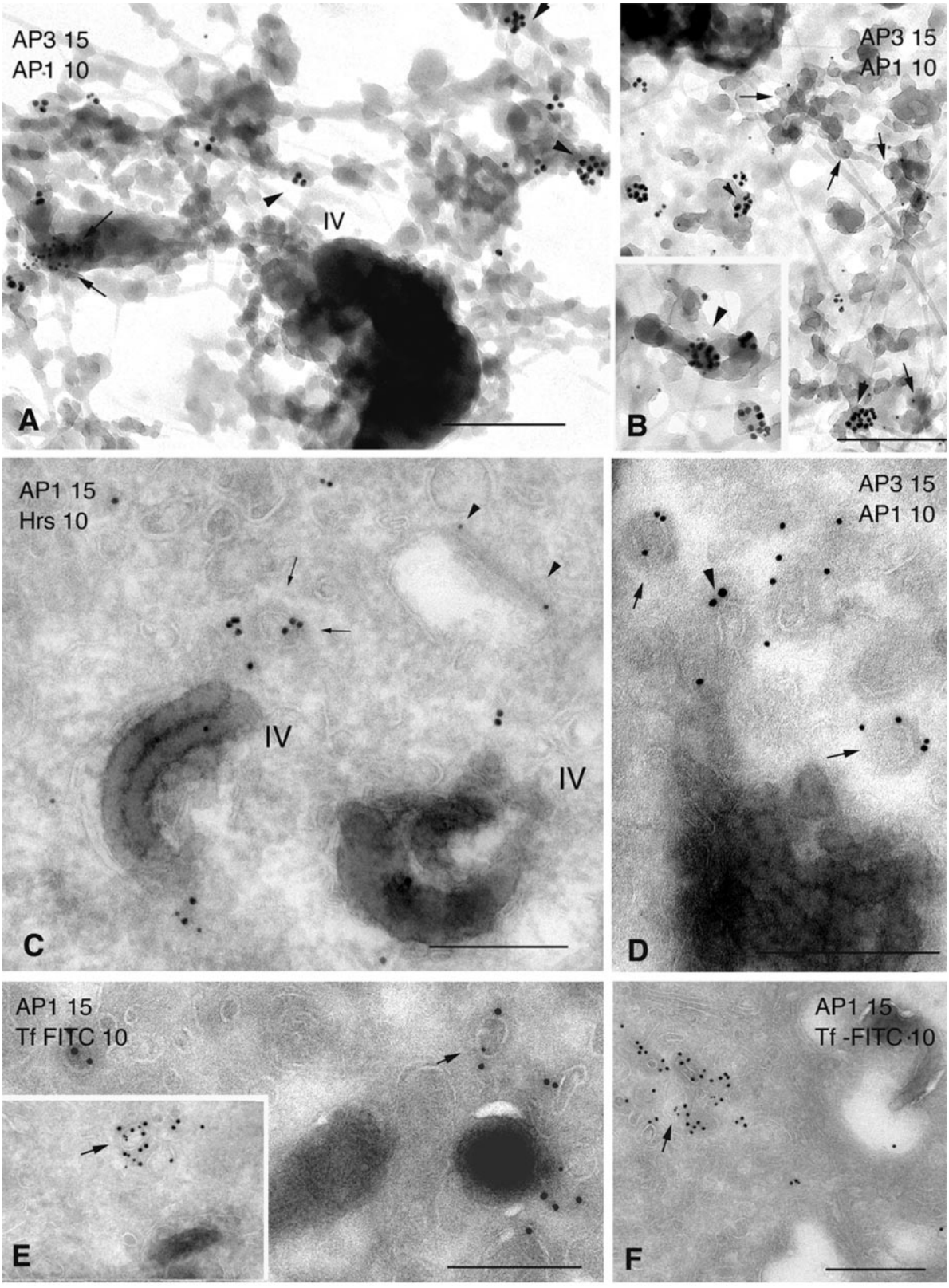

Figure 2. AP-1 and AP-3 are present on distinct endosomal buds in MNT-1 cells. Whole-mount preparations (A and B) and ultrathin cryosections (C–F) of MNT-1 cells were double immunogold labeled as indicated using PAG10 and PAG15. Before immunogold labeling, cells were incubated at 37°C for 1 h with Tf-HRP and then processed for whole-mount cytochemistry (A and B) or with Tf-FITC and then fixed and cryosectioned (E, E inset, and F). Arrowheads indicate labeling for AP-3 (A, B, and D) or Hrs (C). Arrows indicate labeling for AP-1 (A–D) or buds labeled for both AP-1 and Tf-FITC (E and F). Note the predominant labeling for AP-1 near stage IV melanosomes (IV) in A–E and the bud labeled for both AP-1 and AP-3 (B, inset). Bars, 200 nm.

Table 1. Relative distribution (percentage) of AP-3 and AP-1 in melan-a cells

	Golgi	TGN	TVEs/End	TVEs/MVBs	TVEs/Melan	TVEs/Lys	Vesicles/cytoplasm
AP-3	3.5	9.4	41.5	4	25.8	1.8	14
AP-1	0	17.6	39	4	19	1.5	18.5

TVEs, tubulovesicular elements close to endosomal vacuoles (End), melanosomes (Melan), MVBs, and lysosomes (Lys).

Numbers represent the percentages of gold particles labeling AP-3 and AP-1 over the indicated compartments. In total, 450 and 448 gold particles were counted for AP-3 and AP-1, respectively, on randomly selected cell profiles.

to nonmelanosomal compartments (such as endosomes) in addition to melanosomes, and technical limitations of immunofluorescence microscopy for detecting tyrosinase residing in mature melanosomes.

To quantitatively evaluate tyrosinase localization, the antibodies were used for immunogold labeling of ultrathin cryosections of melan-a cells. As shown in Figure 5A and Table 1, tyrosinase is detected primarily in stage III and IV melanosomes, consistent with histochemical analyses for tyrosinase activity using DOPA as a substrate (Yamamoto and Takeuchi, 1981; Zhao *et al*., 1994; Boissy *et al*., 1998; also see Supplemental Figure S4D). Stage II premelanosomes with characteristic internal striations but no pigment are not labeled. Tyrosinase is present predominantly at the limiting membrane of stage III and IV melanosomes, although significant labeling is also often detected on membranes in the lumen of less pigmented stage III melanosomes (Figure 5A and Supplemental Figure S4A). Besides melanosomes, some labeling for tyrosinase, like that for Tyrp1 (Vijayasaradhi *et al*., 1995; Raposo *et al*., 2001) and consistent with previous histochemical analyses (reviewed in Jimbow *et al*., 2000), is detected in the Golgi and in vesicles in the TGN area (Figure 5B). This labeling is seen primarily on noncoated membranes that are distinct from those labeled for the TGN resident protein TGN38 (our unpublished data). Interestingly, more substantial tyrosinase labeling is apparent in endosomal vacuoles and particularly within tubular extensions close to the vacuoles (Figure 5C and Table 2) and in tubules and vesicles closely apposed to melanosomes (Figure 5D). MVBs are not substantially labeled (Supplemental Figure S4C). Quantitative evaluation of the immunogold labeling in the different compartments (Table 2) emphasizes the prevalence of tyrosinase accumulation at steady state within endosomal vacuoles and closely apposed tubules.

Tyrosinase Accumulates in AP-3- and AP-1-enriched Endosomal Domains

To determine whether the tubulovesicular cohort of tyrosinase in melan-a cells was enriched in AP-3-and AP-1-coated regions, ultrathin cryosections were double immunogold labeled. As shown in Figure 6, AP-3-containing tubules and vesicles near both melanosomes and endosomes are also labeled with anti-tyrosinase antibodies (Figures 6, A and B, B inset, and S4A), whereas the bulk of tyrosinase labeling in the TGN area is on uncoated membranes that lack AP-3 (Figure 6C). To evaluate the concentration of tyrosinase in AP-3-positive tubulovesicular elements, we determined the labeling densities of this cargo protein in the different defined areas (Table 3). The enrichment of tyrosinase in AP-3-positive areas was then obtained by dividing the labeling densities in AP-3-positive by those obtained in AP-3-negative areas. These data show that tyrosinase is concentrated in AP-3-coated membranes essentially of endosomal origin.

Consistent with the biochemical interaction of AP-1 and tyrosinase, IEM analysis revealed that tyrosinase is also present in clathrin-coated buds and vesicles that contain AP-1 (Figure 6D). Many of these 80-nm vesicles are close to endosomal tubules and thus resemble the AP-1-coated structures labeled by Tf-FITC in MNT-1 cells (Figure 6D). As described above, in the TGN area, tyrosinase does not seem to be consistently present in coated vesicles (Supplemental Figure S4B). Estimation of the labeling densities for tyrosinase in AP-1-positive and -negative membranes indicated that despite a higher enrichment in AP-3-positive areas, tyrosinase is also consistently concentrated in AP-1-coated elements (Table 3). Therefore, we conclude that the bulk of tyrosinase associates with both AP-1- and AP-3-coated endosomal domains in melanocytes.

Partial Impairment of Tyrosinase Transport from Endosomes to Melanosomes in AP-3-deficient Melanocytes

AP-1 deficiency is embryonically lethal, precluding an assessment of tissue-specific AP-1 functions (Zizioli *et al*., 1999). By contrast, AP-3-deficient mice are viable, but they have defective pigment granule function. If both AP-1 and AP-3 participate in tyrosinase sorting from endosomes, then tyrosinase trafficking should be only partially impaired in the absence of AP-3. To test this prediction, we analyzed the subcellular distribution of tyrosinase in AP-3-deficient melanocytic cells. The immortalized melanocyte cell line melan-pe was derived from homozygous pearl ($Ap3b1^{Pe}$/$Ap3b1^{Pe}$) mice, which bear a truncating mutation in the AP-3 β3A subunit (Feng *et al*., 1999). As shown by immunoblotting, melan-pe cells lack functional AP-3 (note the disappearance of the μ3 and δ subunits in anti-δ immunoprecipitates; Figure 7B), but they contain levels of tyrosinase comparable with those of melan-a cells (Figure 7A). Although the gross distribution of tyrosinase (or other melanosomal markers) in melan-pe cells seems similar to that in melan-a cells by immunofluorescence microscopy analyses (Supplemental Figure S3C), IEM analysis of ultrathin cryosections shows an abnormal accumulation of tyrosinase primarily in enlarged vacuolar endosomes (arrows) with abundant emanating tubules as well as in MVBs (stars) (Figure 7, C and D, and Table 2). The vacuolar compartments are labeled for Hrs, defining them as endosomes (Figure 7C and inset). Much of the labeling for tyrosinase on MVBs coincides with intralumenal vesicles (ILVs), contrasting with the nearly exclusive labeling of the limiting membrane of endosomes in melan-a cells (compare Figure 7D with Figure 5). Similar enlarged vacuolar structures (Figure 7E) and nearby tubulovesicular elements (Figure 7F) are labeled by DOPA histochemistry in standard thick sections of primary melanocytes cultured from homozygous pearl mice, and they are absent in WT controls (Supplemental Figure S4D). These

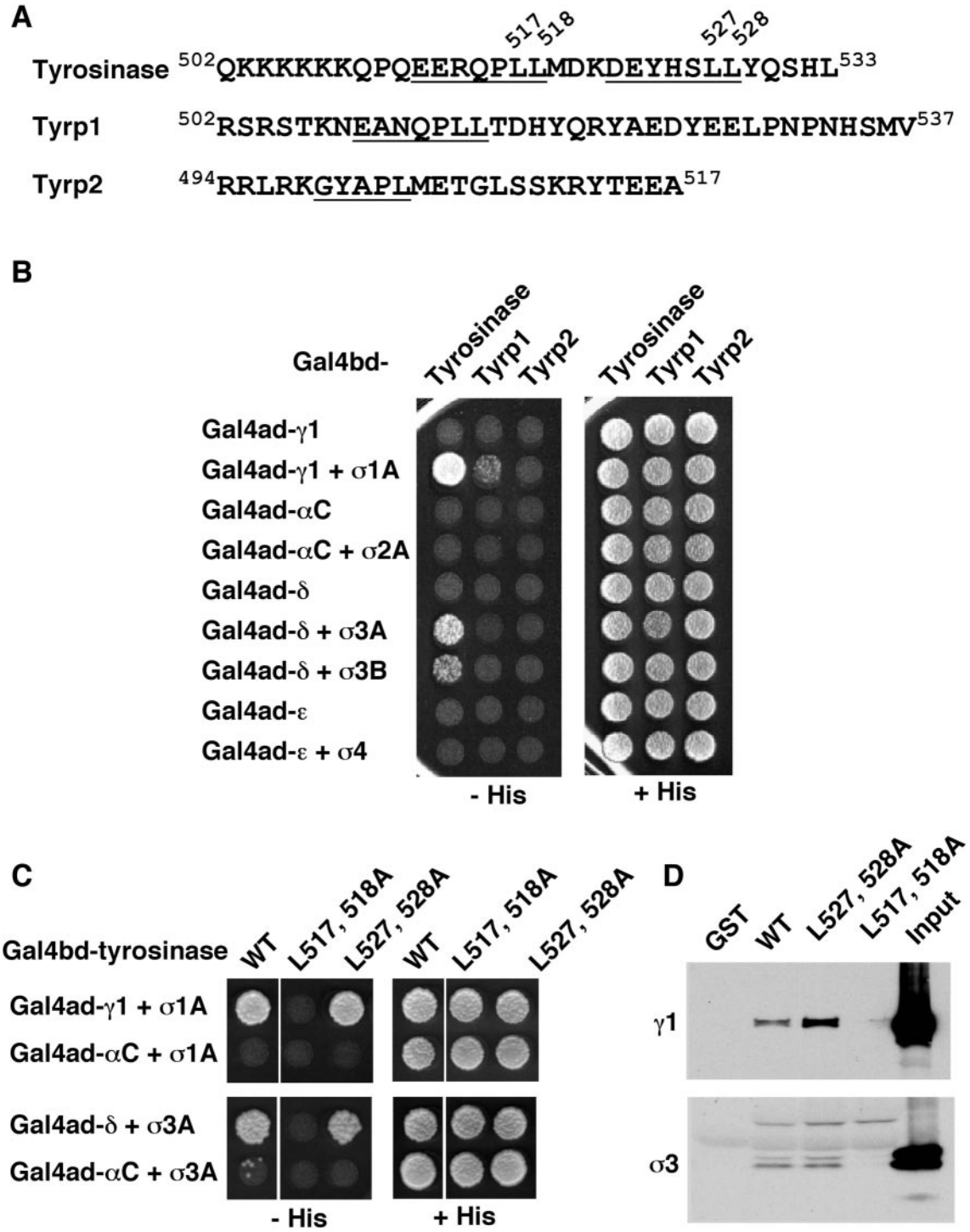

Figure 3. AP-1 and AP-3 bind to the dileucine-based targeting signal of tyrosinase. (A) Sequences of the cytoplasmic domains of mouse tyrosinase, Tyrp1 and Tyrp2. Known or putative dileucine- and tyrosine-based sorting signals and amino acid numbers are indicated. (B) The indicated cytoplasmic domains fused to the Gal4BD were tested in a yeast three-hybrid assay with the Gal4AD fused to the indicated AP heavy chains (γ1 for AP-1, αC for AP-2, δ for AP-3, or ϵ for AP-4) in the absence or presence of the cognate light chains (σ1A, σ2, σ3A, σ3B, or σ4). *S. cerevisiae* HF7c cells transduced with the indicated plasmids were patched onto minimal medium plates with (+His) or without (−His) histidine. Growth in the absence of histidine indicates a positive interaction. (C) Yeast three-hybrid analysis of tyrosinase cytoplasmic domain constructs, fused to the Gal4BD, coexpressed with the σ1A and Gal4AD fused to either γ1 or αC. *S. cerevisiae* HF7c cells transduced with all three plasmids were grown in minimal medium plates with (+His) or without (−His) histidine. The tyrosinase fusions were either WT or site-directed mutants of the indicated leucine residues to alanine. (D) GST or GST fusion proteins containing the WT tyrosinase cytoplasmic domain or site-directed mutants with alanine substitutions at the relevant (L517 and 518A) or irrelevant (L527 and 528A) dileucine sequences were incubated with bovine brain extracts and then precipitated with glutathione-Sepharose. The precipitates were fractionated by SDS-PAGE and probed by immunoblotting with antibodies to the γ1 or σ3 chains of AP-1 and AP-3, respectively. The last lane is a percentage of the input extract for the precipitations. Positions of the relevant chains are noted to the left; σ3 migrates as a doublet.

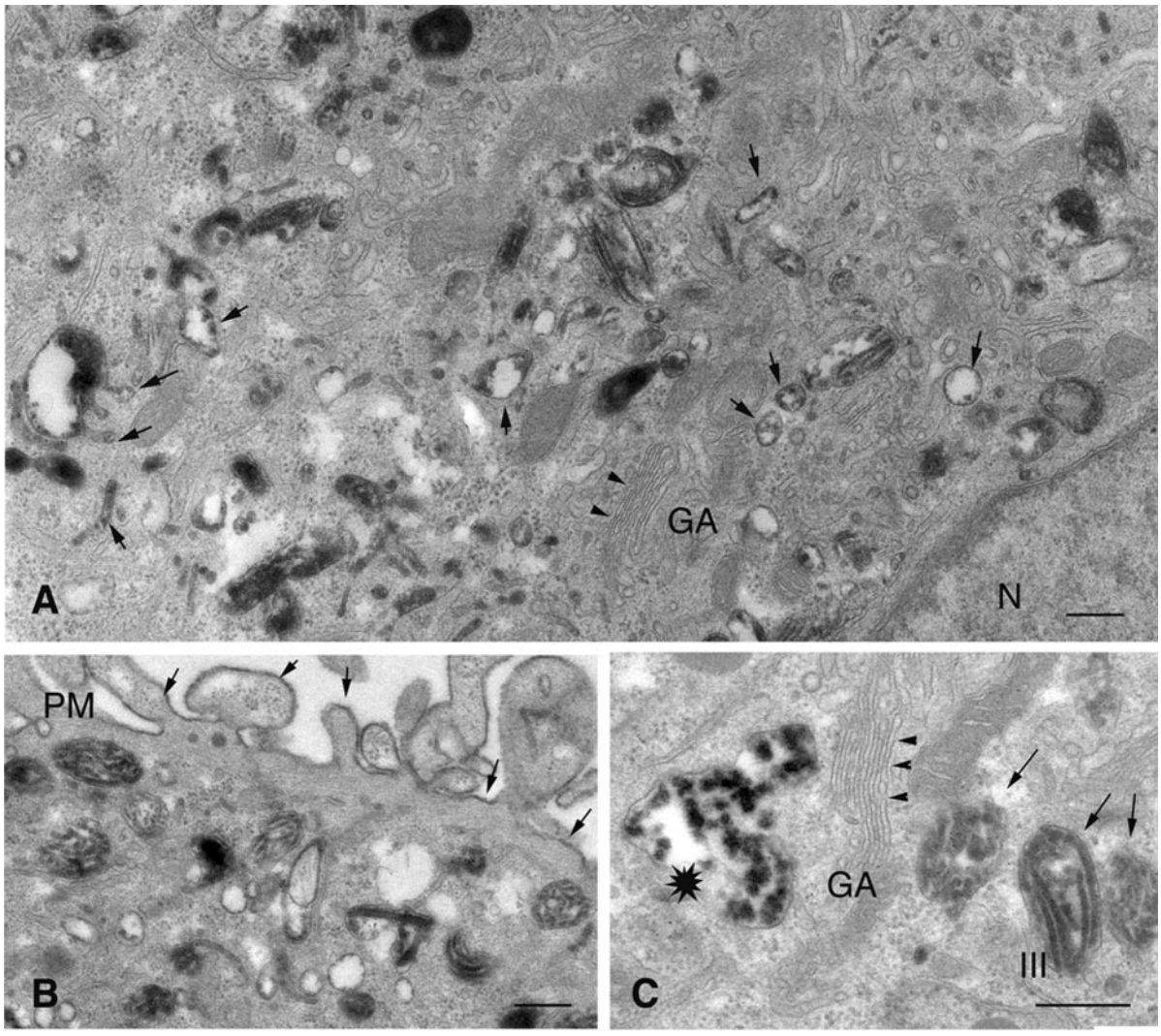

Figure 4. HRP-tyrosinase chimera lacking the dileucine-based signal accumulates downstream of tubular endosomes. MNT-1 cells were transiently transfected with HRP-tyrAA and processed for HRP cytochemistry and Epon embedding. (A) Accumulation of HRP-tyrAA in tubular and vacuolar compartments often showing associated buds (arrows). Note the absence of accumulation of HRP-tyrAA in the Golgi area (arrowheads). (B) HRP-tyrAA is also detected at the plasma membrane (PM) and arrows. (C) HRP-tyrAA is present in compartments with features of MVBs (star) but not in the Golgi (arrowheads) or in melanosomes (arrows). III, stage III melanosomes; GA, Golgi apparatus. Bars, 200 nm.

data indicate that in the absence of AP-3, tyrosinase accumulates in endosomal structures, including vacuoles, tubules, and ILVs of MVBs.

Despite the significant redistribution of tyrosinase, melan-pe cells are pigmented and harbor melanosomes that are indistinguishable from those of WT cells as observed by DOPA histochemical staining and standard EM analyses (Figures 7E and 8A). Moreover, although the distribution of tyrosinase in melan-pe cells largely resembles that of dileucine signal-deficient HRP-tyrAA in MNT-1 cells, it differs in that a reduced but significant fraction of tyrosinase in melan-pe cells remains associated with melanosomes (Table 2), and the cohort of tyrosinase near endosomal vacuoles is enriched in vesicles with clearly visible coats (Figure 7G). This suggests that although AP-3 is responsible for much of tyrosinase transport from tubulovesicular endosomes toward melanosomes, the dileucine signal may additionally drive tyrosinase toward a second AP-3-independent pathway, perhaps mediated by AP-1. Consistent with this prediction, double immunogold labeling of melan-pe cells revealed abundant AP-1-coated vesicles and tubulovesicular elements containing tyrosinase near endosomal vacuoles (Figure 8B). As in melan-a, the AP-1-coated tyrosinase-containing vesicles in melan-pe cells were often observed close to melanosomes (Figure 8C). Quantitation of the labeling reveals that the percentage of AP-1-coated buds and vesicles containing tyrosinase in melan-pe is more than double that in melan-a (49 vs. 22%; Table 4). The labeling density of tyrosinase in AP-1-positive and -negative membranes (see *Materials and Methods*) was 0.46 and 0.06 gold particles/intersection, respectively, which corresponded to a relative enrichment of 7.66 (compared with 5.28 in melan-a cells; Table 3). These observations suggest that tyrosinase is normally sorted within the melanocyte by both AP-1- and AP-3-dependent mechanisms; that in the absence of AP-3, AP-1 "sees" a greater proportion of tyrosinase that would otherwise be preferentially recruited to nascent AP-3-coated do-

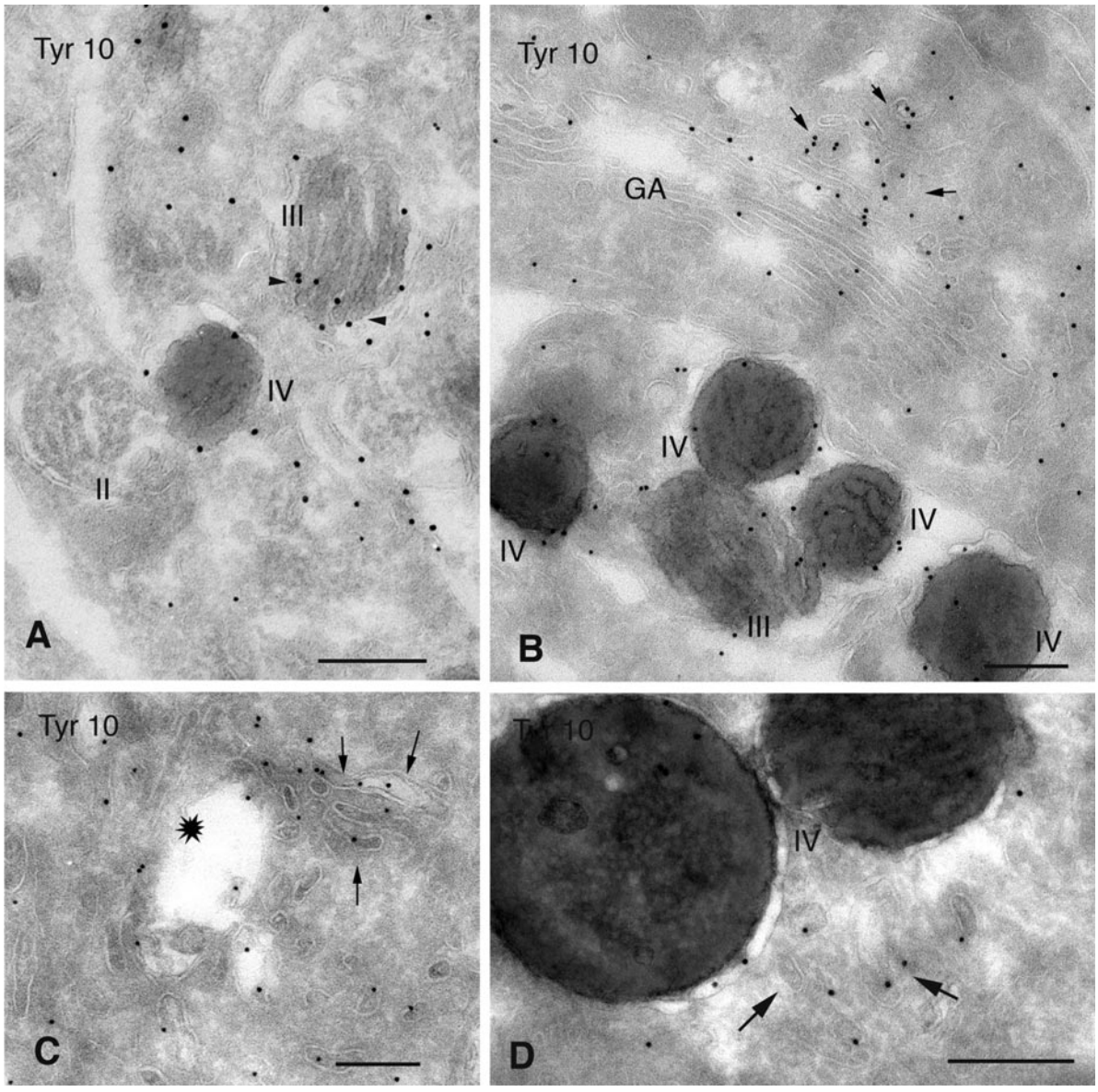

Figure 5. Tyrosinase localizes to tubular structures near endosomal compartments in addition to melanosomes and vesicles in the Golgi area. (A–D) Ultrathin cryosections of melan-a cells were immunogold labeled for tyrosinase with PAG10. (A and B) Tyrosinase labeling the limiting membrane of endosomes and stage III and IV melanosomes. Stage II premelanosomes with characteristic internal striations but no pigment (II) are not labeled. (B) A section emphasizing the Golgi area (GA). Note tyrosinase labeling in Golgi stacks and predominantly uncoated vesicles near the TGN (arrows). (C) Prominent tyrosinase labeling is detected on tubules (arrows) closely apposed to vacuolar endosomes (star). (D) Tyrosinase labeling of tubules (arrows) closely apposed to stage IV melanosomes. Bars, 200 nm.

Table 2. Quantitation of tyrosinase labeling (percentage) in different intracellular compartments

	Golgi	TGN	Endosomes	TVEs/End	MVBs	Melanosomes	TVEs/Melan	Lys	Vesicles
Melan-a	8.7	10.5	10.7	19.7	5.7	28.5	11.0	2.2	3.0
Melan-pe	9.0	12.0	26.5	12.0	20.0	12.0	5.0	3.0	0.5

TVEs, tubulovesicular elements close to endosomal vacuoles (TVEs/End) and melanosomes (TVEs/Melan); Lys, lysosomes.

Results are presented as the percentage of gold particles labeling the distinct defined compartments in melan-a and melan-pe cells. In total, 1033 and 1100 gold particles were counted in randomly selected cell profiles of melan-a and melan-pe, respectively. Melanosomes comprise stage II, III, and IV, and the percentage of tyrosinase in each stage, respectively, is 1, 8.5, and 19% for melan-a, and 0.5, 3, and 8.5% for melan-pe. In both melan-a and melan-pe cells, the highest labeling for tyrosinase is observed in stage IV melanosomes.

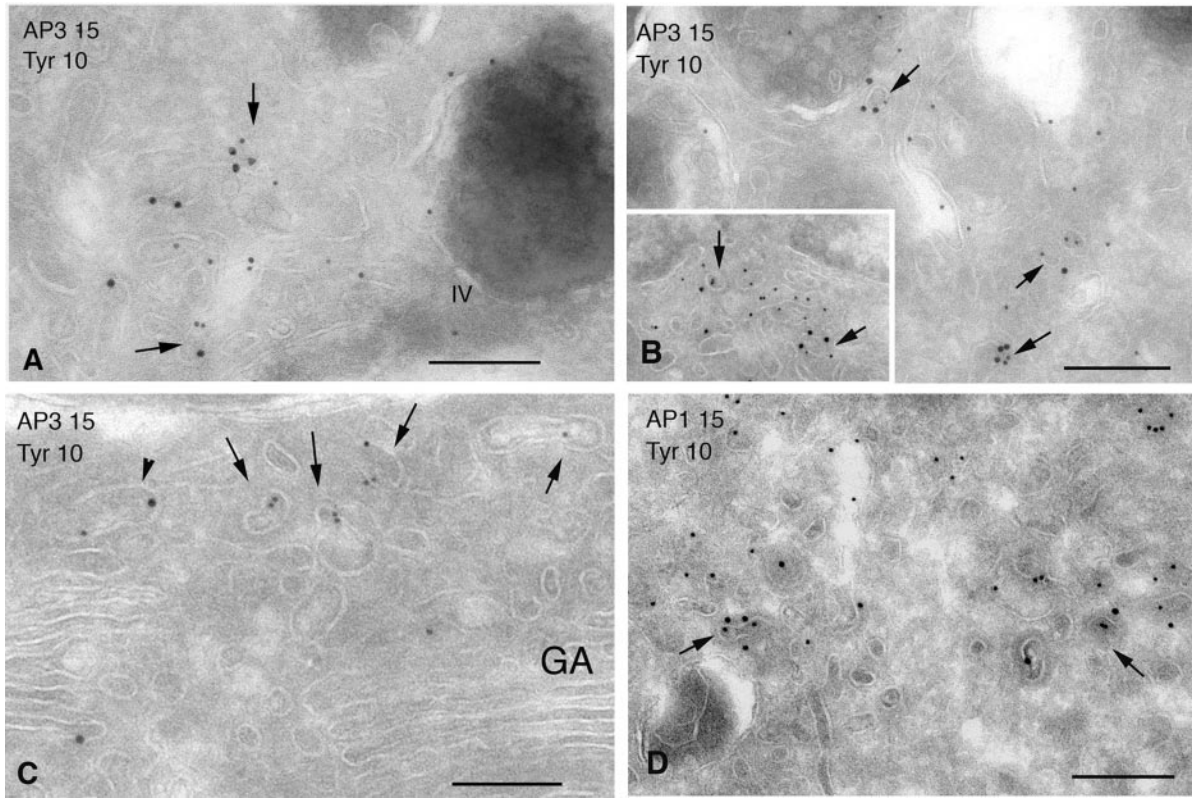

Figure 6. Tyrosinase accumulates in AP-3- and AP-1-enriched endosomal domains. Ultrathin cryosections of melan-a cells were double labeled for tyrosinase (PAG10) and either AP-3 (PAG15; A–C) or AP-1 (PAG15; D). (A and B) Note the AP-3-positive vesicles and tubules containing tyrosinase (arrows) that are close to stage IV melanosomes (A, B, and B inset). (C) Tyrosinase near the Golgi (GA) is found in vesicles that lack apparent coats (arrows) and only infrequently label for AP-3 (C, arrowhead). (D) Tyrosinase and AP-1 coincide in coated vesicles and tubules (arrows). Bars, 200 nm.

mains; and that AP-1 provides an alternative route to the melanosome independent of that mediated by AP-3.

DISCUSSION

Cells harboring LROs use ubiquitously expressed machinery to effect cell type-specific sorting events. We show here that AP-1 and AP-3 both associate on endosomes with tyrosinase and mediate its delivery to melanosomes in distinct but partially redundant pathways. These pathways provide for transport out of early endosomes before or concomitant with endosomal maturation and the generation of MVBs and early stage melanosomes from them. In melanocytes, this mechanism of endosomal export facilitates delivery of tyrosinase at the proper stage during melanosome maturation and "rescues" tyrosinase from being incorporated into maturing MVBs carrying lysosomal cargo. Our data shed light on the trafficking pathways followed by tyrosinase, a key enzyme in melanogenesis, toward melanosomes. Moreover, they have important implications for the general function of both AP-3 and AP-1 in sorting to lysosomes and LROs.

Table 3. Tyrosinase is enriched in AP-3- and AP-1-coated areas of melan-a cells

	Labeling density (gold/intersection)		Ratio AP positive/ AP negative
	Positive	Negative	
AP-3	0.48 ± 0.03	0.05 ± 0.02	9.6
AP-1	0.37 ± 0.04	0.07 ± 0.03	5.28

Numbers represent the labeling densities ± SEM of tyrosinase in AP-3-positive and -negative membranes and in AP-1-positive and AP-1-negative membranes. AP-3- and AP-1-negative (neg) areas included were continuous to the AP-3- and AP-1-positive (pos) membranes.

Figure 7 (facing page). Tyrosinase accumulates in endosomal structures in AP-3-deficient melanocytes. (A and B) Immunoblot analysis of tyrosinase (Tyr; A) and AP-3 subunits δ, β3A, and μ3 (B) in melan-a (a) and melan-pe (pe) cells. Tyrosinase (A) or AP-3 (B) was immunoprecipitated from Triton X-100 lysates of equal numbers of melan-a and melan-pe cells and then fractionated by SDS-PAGE and immunoblotted with the indicated antibodies. Numbers indicate positions of molecular weight markers. (C and D) Ultrathin cryosections of melan-pe cells were double labeled for tyrosinase (PAG15) and Hrs (PAG10) (C) or single labeled for tyrosinase (D). Note the accumulation of tyrosinase on MVBs (stars) and on vacuolar endosomes (arrowheads) labeled for Hrs (arrows in C, inset). (E and F) Melan-pe cells were analyzed by DOPA cytochemistry for tyrosinase activity. Note the accumulation of reaction product in vacuolar endosomes (E and F; see star in F) and tubules associated with these structures (arrows, F) and the Golgi (GA) (E). (G) Melan-pe cells immunogold labeled for tyrosinase with PAG15, emphasizing labeling on vacuolar endosomes (star), associated tubules, and coated vesicles (arrows). Bars, 200 nm.

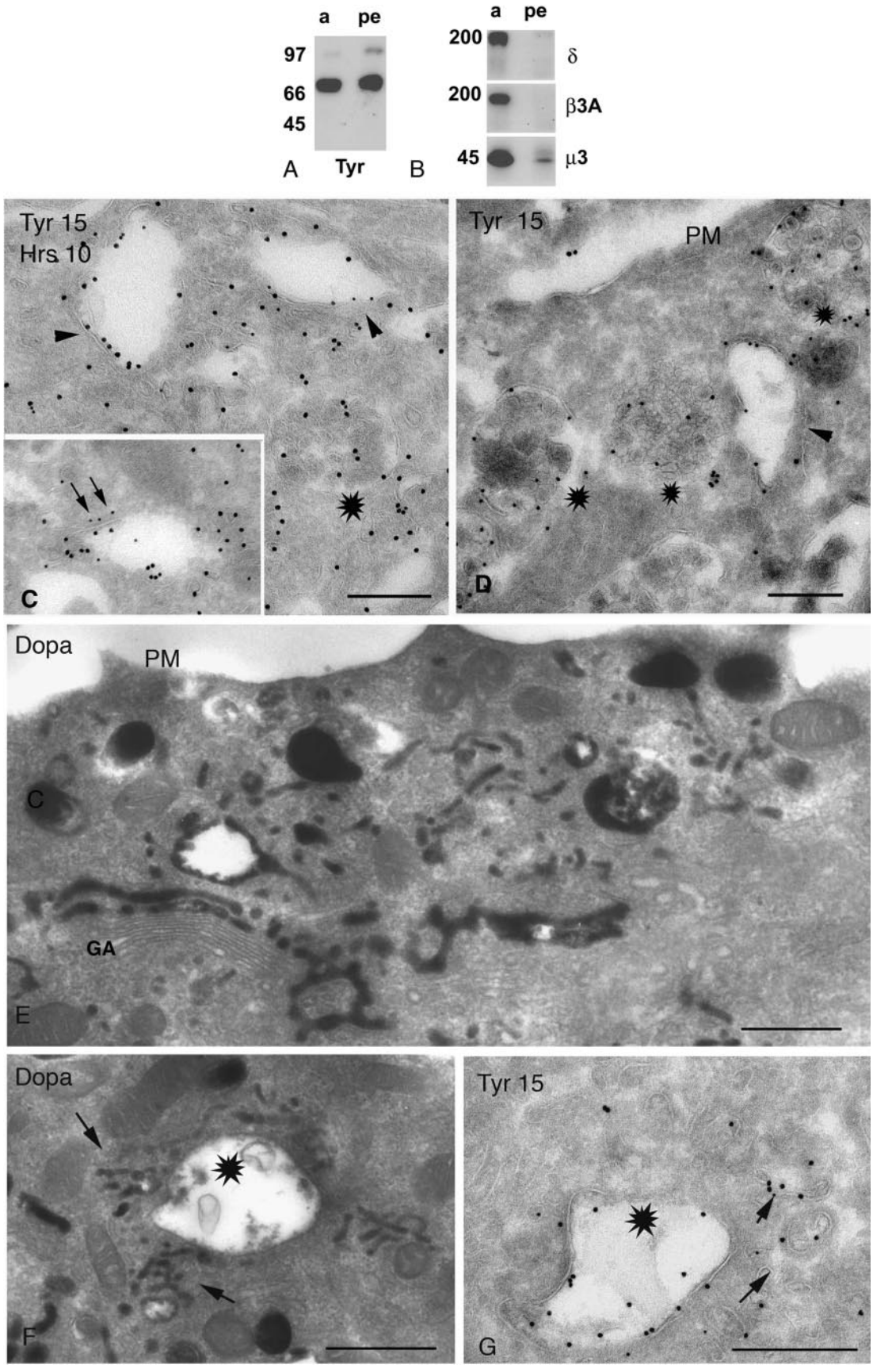
a
pe
97
66
45
A
Tyr
B
200
δ
200
β3A
45
μ3
Tyr 15
Hrs 10
C
Tyr 15
PM
D
Dopa
PM
C
GA
E
Dopa
F
Tyr 15
G

Figure 7.

AP-3 Acts Primarily in Endosomes

We show here using quantitative, high-resolution EM techniques that the main site of accumulation of AP-3 in melanocytic cells is on clathrin-coated buds of early endosomes through which Tf receptors and Pmel17 cycle. Furthermore, loss of AP-3 association, either by mutation of the AP-3-binding signal in HRP-tyrAA or by AP-3 deficiency, correlates with increased accumulation of the AP-3 cargo protein tyrosinase in endosomes. A smaller but significant pool of AP-3 was observed on uncoated membranes near the TGN in melanocytes (our unpublished data), but it was not possible to determine whether these membranes were derived from the TGN or from nearby endocytic tubules. Our results support a quantitative study of AP-3 localization in HepG2 cells (Peden *et al*., 2004) and suggest that 1) the major site of AP-3-dependent protein sorting is at early endosomes, and 2) AP-3 functions to rescue proteins from a default route toward late endosomal MVBs and to sort them toward lysosomes or LROs.

Tyrosinase Sorting from Endosomes

Tyrosinase activity has long been documented in clathrin-coated structures (Orlow, 1998). We show here using quantitative immunogold labeling of mouse tyrosinase that although a fraction can be observed in tubulovesicular structures associated with the Golgi, a much larger fraction is present in clathrin-enriched regions of tubulovesicular endosomes. Many of these structures are near mature melanosomes and are coated with AP-1 or AP-3. These endosomal domains likely represent intermediates in the AP-3- and AP-1-dependent trafficking of tyrosinase toward melanosomes. This is supported for AP-3 by the accumulation of tyrosinase in endocytic compartments in AP-3-deficient melanocytes from congenic pearl mice, shown here, and from human Hermansky Pudlak Syndrome patients (observed by cytochemical EM; Huizing *et al*., 2001), concomitant with a depletion from melanosomes. A direct AP-3-dependent endosome-to-melanosome pathway would explain the selective defect in melanosome biogenesis observed in AP-3-deficient animals and would predict that AP-3 may sort cargo directly from endosomes to LROs in other tissues affected by AP-3 deficiency. Why AP-3 cargo is sorted to melanosomes and not to lysosomes in melanocytes is not yet understood, but it may depend upon cell type-specific distribution of target endosomal SNARE proteins or their regulators, many of which are up-regulated in melanocytes (Wade *et al*., 2001; our unpublished data). Our results highlight the importance of the endocytic pathway in the biogenesis of melanosomes.

Interestingly, by contrast to the enrichment of lysosomal cargo in AP-3-coated buds of HepG2 cells (Peden *et al*., 2004), we were unable to detect an enrichment of the late endosome/lysosome resident LAMP-1 in AP-3-coated buds of melanocytic cells (our unpublished data). This supports potential cell type specificity in cargo trafficking patterns and the incomplete dependence of LAMP-1 sorting on AP-3 (reflected by the steady-state localization of LAMP-1 to lysosomes in AP-3-deficient cells; Starcevic *et al*., 2002) and by the steady-state redistribution of LAMP-1 upon depletion of AP-2, but not AP-3 or AP-1, in HeLa cells; Janvier and Bonifacino, 2005). Indeed, the trafficking pathways followed by LAMP-1 in melanocytes have yet to be addressed and are beyond the scope of the current study.

Tyrosinase accumulated abnormally in AP-3-deficient cells on vacuolar endosomes and ILVs of MVBs. This further suggests that AP-3 functions to divert cargo from entering into the "classical" Hrs/ESCRT-dependent MVB pathway in mammalian cells (Babst, 2005), a function that would be analogous to that of yeast AP-3. Melanocytes might profit from such a mechanism by 1) ensuring that tyrosinase is removed from the endosomal precursors of stage II melanosomes (Berson *et al*., 2001; Raposo *et al*., 2001) and delivered to stage II melanosomes only after they are fully formed, and 2) preventing tyrosinase partitioning to ILVs within these endosomal precursors and its subsequent default delivery to late endosomes. The missorting of tyrosinase to endosomal ILVs in AP-3-deficient melanocytes may reflect its tendency to associate with invaginating membranes in later compartments, supported by the presence of tyrosinase on internal membranes in stage III melanosomes. A similar AP-3-dependent mechanism in cell types that lack LROs may, by allowing cargo proteins to bypass ESCRT-dependent ILV association in earlier endocytic compartments, provide a means to either avoid ILVs altogether or follow an alternative route to ILVs during later endosome maturation. Thus, the melanosome system may reveal a general property of AP-3-dependent sorting events.

A role for AP-1 in Tyrosinase Sorting

Using yeast three-hybrid and GST pull-down assays, we show for the first time that the cytoplasmic dileucine-based sorting signal of tyrosinase binds not only to the δ-σ3 hemicomplexes of AP-3, confirming an AP-3 interaction (Honing *et al*., 1998) but also to the γ1-σ1A hemicomplex of AP-1. Dual binding to AP-3 and AP-1 has also been observed for dileucine-based signals of HIV-1 Nef, LimpII, and CLN3 (Janvier *et al*., 2003; Kyttala *et al*., 2005). The interaction of the tyrosinase and LimpII signals with AP-1 by yeast three-hybrid assays was not observed in surface plasmon resonance analyses (Honing *et al*., 1998), but it is supported by GST pull-down assays (Figure 3B; Janvier *et al*., 2003) and by earlier biochemical data (Kobayashi *et al*., 1994) in which tyrosinase was enriched in clathrin-coated vesicle fractions that are typically devoid of AP-3 (Dell'Angelica *et al*., 1997; Simpson *et al*., 1997). The importance of this interaction was confirmed by the extensive colocalization of tyrosinase on endosomal buds with AP-1 in melan-a cells, by the dramatic increase in the degree of AP-1/tyrosinase colocalization in AP-3-deficient melanocytes, and by the more dramatic effect on steady state distribution of the dileucine mutation (in HRP-tyr) relative to AP-3 depletion. Note that whereas the tyrosinase cytoplasmic domain shows an apparently stronger interaction with the γ1-σ1A hemicomplex than with the δ-σ3 hemicomplexes in the yeast three-hybrid assay, this may not reflect a stronger in vivo interaction because the assay is sensitive to the degree of folding of hemicomplex subunits.

AP-1-containing endosomal buds were largely nonoverlapping with nearby buds containing AP-3, thus defining two separate adaptor-enriched domains on endosomes. The data suggest that AP-1 participates normally in an AP-3-independent physiological sorting pathway for tyrosinase, and that this pathway becomes the "default" in the absence of AP-3. The existence of such a pathway may explain the continued delivery of tyrosinase to melanosomes in AP-3-deficient melanocytes and the partial pigmentation of AP-3-deficient animals (Lane and Deol, 1974). Tyrp1, which binds AP-1 but not AP-3 by yeast three-hybrid assay and is enriched in AP-1-coated vesicles (Raposo *et al*., 2001), may be an exclusive cargo of the AP-1-dependent pathway, and other melanosomal cargo, analogous to neuronal ion transporters (Salazar *et al*., 2004), may exclusively use an AP-3-dependent pathway.

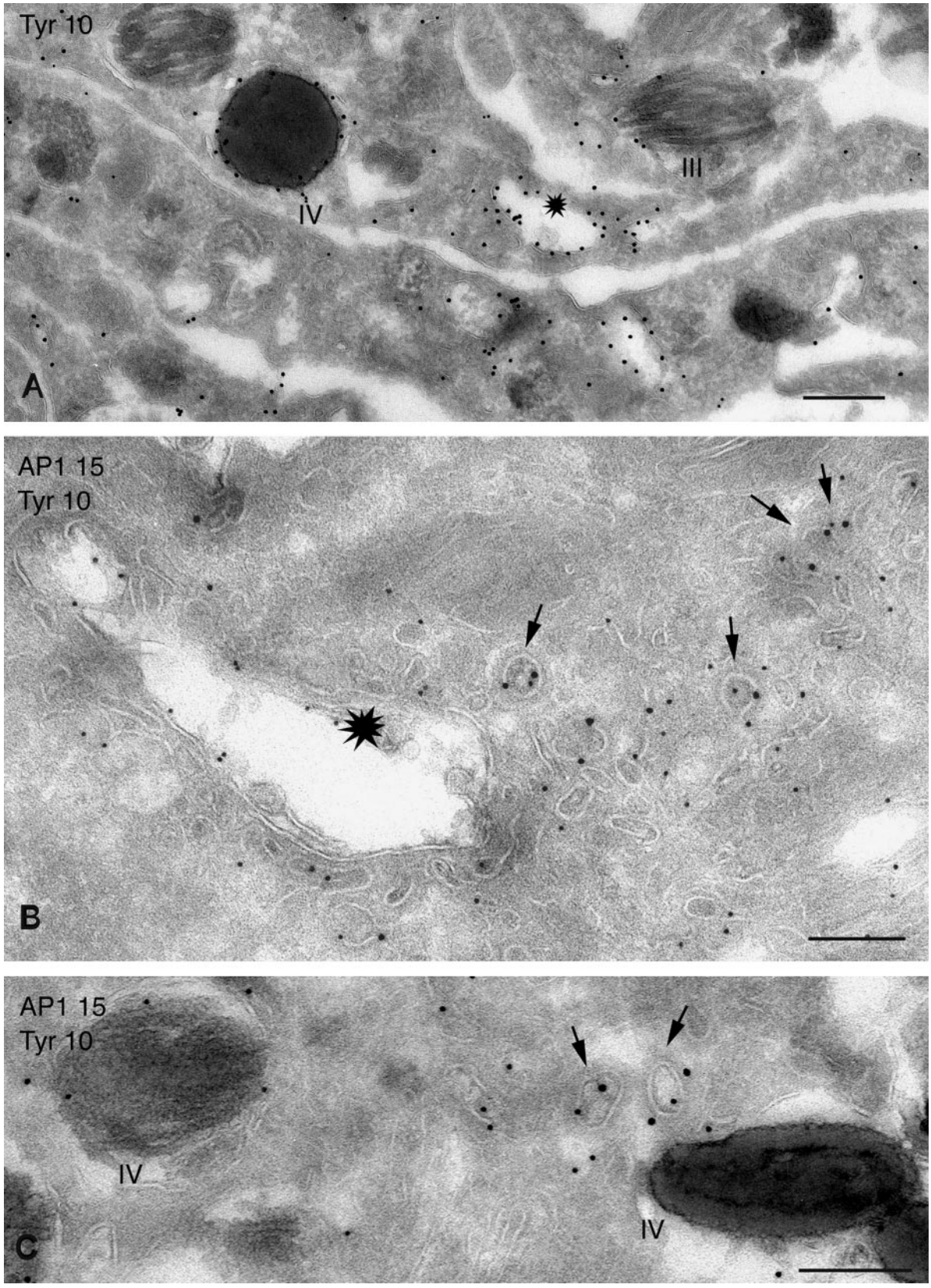

Figure 8. Increased association of tyrosinase with AP-1 in AP-3-deficient melanocytes. Ultrathin cryosections of melan-pe cells were immunogold labeled for tyrosinase alone (PAG10; A) or with AP-1 (PAG15; B and C). Note that stage III and IV melanosomes are present within melan-pe cells and that tyrosinase labeling can be observed on them (A and C) in addition to the vacuolar endosomes (star). Coincidence of labeling for AP-1 and tyrosinase (B and C, arrows) is observed at high levels on coated tubules and vesicles near vacuolar endosomes (B, star) and melanosomes (C, IV). Bars, 200 nm.

Table 4. Quantitation of AP-3- and AP-1-labeled buds and vesicles that also contain tyrosinase in melan-a and melan-pe

	Buds and vesicles (%)			
Cell type	AP-3/ Tyr-neg	AP-3/ Tyr-pos	AP-1/ Tyr-neg	AP-1/ Tyr-pos
Melan-a	68	32	78	22
Melan-pe	ND	ND	51	49

ND, not determined.

Results are presented as percentage of a total of AP-3- or AP-1-labeled structures that are (Tyr-pos) or are not (Tyr-neg) double labeled for tyrosinase in melan-a and melan-pe cells. These data represent a global relative quantitation on all membranes and not only endosomes. For example, tyrosinase is largely absent from the AP-3-coated vesicles and buds in the TGN area. The tyrosinase-negative, AP-3/AP-1-positive vesicles may reflect these structures, cargo diversity of adaptor-coated vesicles, and/or the underestimation of colocalization due to technical limitations (such as steric hindrance of antibodies and gold and epitope destruction by fixation).

AP-3 and AP-1 Cooperation on Endosomes

How can two adaptors participate in melanosomal delivery of tyrosinase? The increased endosomal accumulation of tyrosinase in AP-3-deficient cells suggests that tyrosinase, like LAMP-1 in HepG2 cells (Peden *et al*., 2004), is sorted by AP-3 at the limiting membrane of early endosomes. The tubules associated with AP-3-enriched buds contain Tf and Pmel17, cargo destined from the vacuolar endosomal domains for both recycling to the plasma membrane and incorporation into ILVs (Raposo *et al*., 2001). Thus, we propose that AP-3 removes endocytic cargo before or concomitant with arrival at the vacuolar domain of early endosomes. Cargo that fails to be sequestered by AP-3 will remain in the vacuolar domain, from which it may subsequently be incorporated in the invaginating membranes. This model parallels that of yeast AP-3 in averting the MVB pathway, is likely to be shared by nonspecialized cells that lack LROs, and would explain the enrichment of tyrosinase on internal membranes of MVBs in AP-3-deficient melanocytes. Cargo that remains on the limiting membrane of early endosomes and that is not immediately retained by AP-3 coats or sorted to ILVs in the vacuolar domains may be "rescued" by recruitment into AP-1-coated domains. The incomplete "rescue" of tyrosinase away from ILVs in melan-pe cells might reflect relative inefficiency of AP-1 recruitment due to a lower affinity for AP-1 than for AP-3 (despite the apparent higher affinity observed in the yeast three-hybrid assay) or saturation of the AP-1-dependent pathway by cargo that would preferentially be sorted by AP-3, or perhaps the possibility that AP-1 acts primarily at a different site, on tubules downstream of the vacuolar domain. The destination for cargo recruited into AP-1-coated vesicles is also not clear. These vesicles may be targeted directly to maturing melanosomes, consistent with models of AP-1 function in lysosomal targeting (Honing *et al*., 1996; Klumperman *et al*., 1998; Reusch *et al*., 2002; Kyttala *et al*., 2005) and the proximity of endosomal AP-1-positive buds and vesicles to melanosomes. Alternatively, AP-1 cargo may be destined to recycle back to either the plasma membrane or to the TGN to undergo a second "attempt" at delivery to melanosomes via AP-3 on endosomes or a third uncharacterized pathway (such as transient fusion with multivesicular late endosomes), consistent with the model of AP-1 as a recycling adaptor (Mallard *et al*., 1998; Meyer *et al*., 2000; Crump *et al*., 2001; Valdivia *et al*., 2002). Despite these unresolved questions, what is now clear is that AP-3 and AP-1 function in partially redundant pathways leading from tubular endosomes ultimately to melanosomes. Further elucidation of these pathways should provide more detailed information about the plasticity of the endocytic pathway of all cells and the adaptation of the endocytic pathway for biogenesis of LROs.

ACKNOWLEDGMENTS

We thank Sylvie Urbé, Sharon Tooze, and Frances Brodsky for generous gifts of antibodies. We are grateful to Terry M. Mayhew (University of Nottingham, Nottingham, United Kingdom) for advice on quantitative analysis on immunogold-labeled sections. This work was supported by grants from the Wellcome Trust (to A.A.P. and M.S.R.) and the Medical Research Council (to D.F.C. and M.S.R.), National Institutes of Health Grants EY015625 and AR048155 (to M.S.M., G. R., and A.C.T.), Institut Curie, Centre National de la Recherche Scientifique, and Vaincre les Maladies Lysosomales (to G. R.). A.C.T. was supported by a Medical Research Council Studentship and T32 CA 09140 National Institutes of Health/National Cancer Institute Training Program.

REFERENCES

Acton, S. L., Wong, D. H., Parham, P., Brodsky, F. M., and Jackson, A. P. (1993). Alteration of clathrin light chain expression by transfection and gene disruption. Mol. Biol. Cell *4*, 647–660.

Babst, M. (2005). A protein's final ESCRT. Traffic *6*, 2–9.

Bennett, D. C., Cooper, P. J., and Hart, I. R. (1987). A line of non-tumorigenic mouse melanocytes, syngeneic with the B16 melanoma and requiring a tumour promoter for growth. Int. J. Cancer *39*, 414–418.

Berson, J. F., Harper, D. C., Tenza, D., Raposo, G., and Marks, M. S. (2001). Pmel17 initiates premelanosome morphogenesis within multivesicular bodies. Mol. Biol. Cell *12*, 3451–3464.

Berson, J. F., Theos, A. C., Harper, D. C., Tenza, D., Raposo, G., and Marks, M. S. (2003). Proprotein convertase cleavage liberates a fibrillogenic fragment of a resident glycoprotein to initiate melanosome biogenesis. J. Cell Biol. *161*, 521–533.

Blagoveshchenskaya, A. D., Hewitt, E. W., and Cutler, D. F. (1999). Di-leucine signals mediate targeting of tyrosinase and synaptotagmin to synaptic-like microvesicles within PC12 cells. Mol. Biol. Cell *10*, 3979–3990.

Blott, E. J., and Griffiths, G. M. (2002). Secretory lysosomes. Nat. Rev. Mol. Cell. Biol. *3*, 122–131.

Boehm, M., and Bonifacino, J. S. (2002). Genetic analyses of adaptin function from yeast to mammals. Gene *286*, 175–186.

Boissy, R. E., Zhao, Y., and Gahl, W. A. (1998). Altered protein localization in melanocytes from Hermansky-Pudlak syndrome: support for the role of the HPS gene product in intracellular trafficking. Lab. Invest. *78*, 1037–1048.

Bonifacino, J. S., and Traub, L. M. (2003). Signals for sorting of transmembrane proteins to endosomes and lysosomes. Annu. Rev. Biochem. *72*, 395–447.

Burd, C. G., Babst, M., and Emr, S. D. (1998). Novel pathways, membrane coats and PI kinase regulation in yeast lysosomal trafficking. Semin. Cell Dev. Biol. *9*, 527–533.

Calvo, P. A., Frank, D. W., Bieler, B. M., Berson, J. F., and Marks, M. S. (1999). A cytoplasmic sequence in human tyrosinase defines a second class of di-leucine-based sorting signals for late endosomal and lysosomal delivery. J. Biol. Chem. *274*, 12780–12789.

Crump, C. M., Xiang, Y., Thomas, L., Gu, F., Austin, C., Tooze, S. A., and Thomas, G. (2001). PACS-1 binding to adaptors is required for acidic cluster motif-mediated protein traffic. EMBO J. *20*, 2191–2201.

Dell'Angelica, E. C., Mullins, C., Caplan, S., and Bonifacino, J. S. (2000). Lysosome-related organelles. FASEB J. *14*, 1265–1278.

Dell'Angelica, E. C., Ohno, H., Ooi, C. E., Rabinovich, E., Roche, K. W., and Bonifacino, J. S. (1997). AP-3, an adaptor-like protein complex with ubiquitous expression. EMBO J. *16*, 917–928.

Dell'Angelica, E. C., Shotelersuk, V., Aguilar, R. C., Gahl, W. A., and Bonifacino, J. S. (1999). Altered trafficking of lysosomal proteins in Hermansky-Pudlak syndrome due to mutations in the beta 3A subunit of the AP-3 adaptor. Mol. Cell *3*, 11–21.

Dittie, A. S., Hajibagheri, N., and Tooze, S. A. (1996). The AP-1 adaptor complex binds to immature secretory granules from PC12 cells, and is regulated by ADP-ribosylation factor. J. Cell Biol. *132*, 523–536.

Feng, L., *et al*. (1999). The beta3A subunit gene (Ap3b1) of the AP-3 adaptor complex is altered in the mouse hypopigmentation mutant pearl, a model for Hermansky-Pudlak syndrome and night blindness. Hum. Mol. Genet. *8*, 323–330.

Griffiths, G. (1993). Fine Structure Immunocytochemistry, New York: Springer-Verlag.

Honing, S., Griffith, J., Geuze, H. J., and Hunziker, W. (1996). The tyrosine-based lysosomal targeting signal in lamp-1 mediates sorting into Golgi-derived clathrin-coated vesicles. EMBO J. *15*, 5230–5239.

Honing, S., Sandoval, I. V., and von Figura, K. (1998). A di-leucine-based motif in the cytoplasmic tail of LIMP-II and tyrosinase mediates selective binding of AP-3. EMBO J. *17*, 1304–1314.

Huizing, M., Sarangarajan, R., Strovel, E., Zhao, Y., Gahl, W. A., and Boissy, R. E. (2001). AP-3 mediates tyrosinase but not TRP-1 trafficking in human melanocytes. Mol. Biol. Cell *12*, 2075–2085.

Ihrke, G., Kyttala, A., Russell, M. R., Rous, B. A., and Luzio, J. P. (2004). Differential use of two AP-3-mediated pathways by lysosomal membrane proteins. Traffic *5*, 946–962.

Janvier, K., and Bonifacino, J. S. (2005). Role of the endocytic machinery in the sorting of lysosome-associated membrane proteins. Mol. Biol. Cell *16*, 4231–4242.

Janvier, K., Kato, Y., Boehm, M., Rose, J. R., Martina, J. A., Kim, B. Y., Venkatesan, S., and Bonifacino, J. S. (2003). Recognition of dileucine-based sorting signals from HIV-1 Nef and LIMP-II by the AP-1 gamma-sigma1 and AP-3 delta-sigma3 hemicomplexes. J. Cell Biol. *163*, 1281–1290.

Jimbow, K., Park, J. S., Kato, F., Hirosaki, K., Toyofuku, K., Hua, C., and Yamashita, T. (2000). Assembly, target-signaling and intracellular transport of tyrosinase gene family proteins in the initial stage of melanosome biogenesis. Pigment Cell Res. *13*, 222–229.

Klumperman, J., Kuliawat, R., Griffith, J. M., Geuze, H. J., and Arvan, P. (1998). Mannose 6-phosphate receptors are sorted from immature secretory granules via adaptor protein AP-1, clathrin, and syntaxin 6-positive vesicles. J. Cell Biol. *141*, 359–371.

Kobayashi, T., Urabe, K., Orlow, S. J., Higashi, K., Imokawa, G., Kwon, B. S., Potterf, B., and Hearing, V. J. (1994). The Pmel 17/silver locus protein. Characterization and investigation of its melanogenic function. J. Biol. Chem. *269*, 29198–29205.

Kushimoto, T., Basrur, V., Valencia, J., Matsunaga, J., Vieira, W. D., Ferrans, V. J., Muller, J., Appella, E., and Hearing, V. J. (2001). A model for melanosome biogenesis based on the purification and analysis of early melanosomes. Proc. Natl. Acad. Sci. USA *98*, 10698–10703.

Kyttala, A., Yliannala, K., Schu, P., Jalanko, A., and Luzio, J. P. (2005). AP-1 and AP-3 facilitate lysosomal targeting of batten disease protein CLN3 via its dileucine motif. J. Biol. Chem. *280*, 10277–10283.

Lane, P. W., and Deol, M. S. (1974). Mocha, a new coat color and behavior mutation on chromosome 10 of the mouse. J. Hered. *65*, 362–364.

Lui-Roberts, W. W., Collinson, L. M., Hewlett, L. J., Michaux, G., and Cutler, D. F. (2005). An AP-1/clathrin coat plays a novel and essential role in forming the Weibel-Palade bodies of endothelial cells. J. Cell Biol. *170*, 627–636.

Mallard, F., Antony, C., Tenza, D., Salamero, J., Goud, B., and Johannes, L. (1998). Direct pathway from early/recycling endosomes to the Golgi apparatus revealed through the study of shiga toxin B-fragment transport. J. Cell Biol. *143*, 973–990.

Meyer, C., Zizioli, D., Lausmann, S., Eskelinen, E. L., Hamann, J., Saftig, P., von Figura, K., and Schu, P. (2000). mu1A-adaptin-deficient mice: lethality, loss of AP-1 binding and rerouting of mannose 6-phosphate receptors. EMBO J. *19*, 2193–2203.

Nguyen, T., Novak, E. K., Kermani, M., Fluhr, J., Peters, L. L., Swank, R. T., and Wei, M. L. (2002). Melanosome morphologies in murine models of Hermansky-Pudlak syndrome reflect blocks in organelle development. J. Invest. Dermatol. *119*, 1156–1164.

Odorizzi, G., Cowles, C. R., and Emr, S. D. (1998). The AP-3 complex: a coat of many colours. Trends Cell Biol. *8*, 282–288.

Orlow, S. J. (1998). The biogenesis of melanosomes. In: The Pigmentary System: Physiology and Pathophysiology. ed. J. M. Nordlund, R. E. Boissy, U. J. Hearing, R. A. King, and J. P. Ortanne, New York: Oxford University Press, 97–106.

Page, L. J., and Robinson, M. S. (1995). Targeting signals and subunit interactions in coated vesicle adaptor complexes. J. Cell Biol. *131*, 619–630.

Peden, A. A., Oorschot, V., Hesser, B. A., Austin, C. D., Scheller, R. H., and Klumperman, J. (2004). Localization of the AP-3 adaptor complex defines a novel endosomal exit site for lysosomal membrane proteins. J. Cell Biol. *164*, 1065–1076.

Peden, A. A., Rudge, R. E., Lui, W. W., and Robinson, M. S. (2002). Assembly and function of AP-3 complexes in cells expressing mutant subunits. J. Cell Biol. *156*, 327–336.

Raposo, G., Kleijmeer, M. J., Posthuma, G., Slot, J. W., and Geuze, H. J. (1997). Immunogold labeling of ultrathin cryosections: application in immunology. In: Handbook of Experimental Immunology, Vol. 4, ed. L. A. Herzenberg, D. Weir, L. A. Herzenberg, and C. Blackwell, Cambridge, MA: Blackwell Science, 1–11.

Raposo, G., Tenza, D., Murphy, D. M., Berson, J. F., and Marks, M. S. (2001). Distinct protein sorting and localization to premelanosomes, melanosomes, and lysosomes in pigmented melanocytic cells. J. Cell Biol. *152*, 809–824.

Reusch, U., Bernhard, O., Koszinowski, U., and Schu, P. (2002). AP-1A and AP-3A lysosomal sorting functions. Traffic *3*, 752–761.

Reynolds, E. S. (1963). The use of lead citrate at high pH as an electron-opaque stain in electron microscopy. J. Cell Biol. *17*, 208–212.

Robinson, M. S. (2004). Adaptable adaptors for coated vesicles. Trends Cell Biol. *14*, 167–174.

Robinson, M. S., and Bonifacino, J. S. (2001). Adaptor-related proteins. Curr. Opin. Cell Biol. *13*, 444–453.

Rous, B. A., Reaves, B. J., Ihrke, G., Briggs, J. A., Gray, S. R., Stephens, D. J., Banting, G., and Luzio, J. P. (2002). Role of adaptor complex AP-3 in targeting wild-type and mutated CD63 to lysosomes. Mol. Biol. Cell *13*, 1071–1082.

Sachse, M., Urbe, S., Oorschot, V., Strous, G. J., and Klumperman, J. (2002). Bilayered clathrin coats on endosomal vacuoles are involved in protein sorting toward lysosomes. Mol. Biol. Cell *13*, 1313–1328.

Salazar, G., Love, R., Styers, M. L., Werner, E., Peden, A., Rodriguez, S., Gearing, M., Wainer, B. H., and Faundez, V. (2004). AP-3-dependent mechanisms control the targeting of a chloride channel (ClC-3) in neuronal and non-neuronal cells. J. Biol. Chem. *279*, 25430–25439.

Seaman, M. N., Sowerby, P. J., and Robinson, M. S. (1996). Cytosolic and membrane-associated proteins involved in the recruitment of AP-1 adaptors onto the trans-Golgi network. J. Biol. Chem. *271*, 25446–25451.

Seiji, M., Shimao, K., Birbeck, M. S., and Fitzpatrick, T. B. (1963). Subcellular localization of melanin biosynthesis. Ann. NY. Acad. Sci. *100*, 497–533.

Seong, E., Wainer, B. H., Hughes, E. D., Saunders, T. L., Burmeister, M., and Faundez, V. (2005). Genetic analysis of the neuronal and ubiquitous AP-3 adaptor complexes reveals divergent functions in brain. Mol. Biol. Cell *16*, 128–140.

Simmen, T., Schmidt, A., Hunziker, W., and Beermann, F. (1999). The tyrosinase tail mediates sorting to the lysosomal compartment in MDCK cells via a di-leucine and a tyrosine-based signal. J. Cell Sci. *112*, 45–53.

Simpson, F., Bright, N. A., West, M. A., Newman, L. S., Darnell, R. B., and Robinson, M. S. (1996). A novel adaptor-related protein complex. J. Cell Biol. *133*, 749–760.

Simpson, F., Peden, A. A., Christopoulou, L., and Robinson, M. S. (1997). Characterization of the adaptor-related protein complex, AP-3. J. Cell Biol. *137*, 835–845.

Starcevic, M., Nazarian, R., and Dell'Angelica, E. C. (2002). The molecular machinery for the biogenesis of lysosome-related organelles: lessons from Hermansky-Pudlak syndrome. Semin. Cell Dev. Biol. *13*, 271–278.

Stinchcombe, J., Bossi, G., and Griffiths, G. M. (2004). Linking albinism and immunity: the secrets of secretory lysosomes. Science *305*, 55–59.

Stoorvogel, W., Oorschot, V., and Geuze, H. J. (1996). A novel class of clathrin-coated vesicles budding from endosomes. J. Cell Biol. *132*, 21–33.

Sviderskaya, E. V., Bennett, D. C., Ho, L., Bailin, T., Lee, S. T., and Spritz, R. A. (1997). Complementation of hypopigmentation in p-mutant (pink-eyed dilution) mouse melanocytes by normal human P cDNA, and defective complementation by OCA2 mutant sequences. J. Invest. Dermatol. *108*, 30–34.

Valdivia, R. H., Baggott, D., Chuang, J. S., and Schekman, R. W. (2002). The yeast clathrin adaptor protein complex 1 is required for the efficient retention of a subset of late Golgi membrane proteins. Dev. Cell *2*, 283–294.

Vijayasaradhi, S., Xu, Y., Bouchard, B., and Houghton, A. N. (1995). Intracellular sorting and targeting of melanosomal membrane proteins: identification of signals for sorting of the human brown locus protein, gp75. J. Cell Biol. *130*, 807–820.

Wade, N., Bryant, N. J., Connolly, L. M., Simpson, R. J., Luzio, J. P., Piper, R. C., and James, D. E. (2001). Syntaxin 7 complexes with mouse Vps10p tail

interactor 1b, Syntaxin 6, vesicle-associated membrane protein (VAMP)8, and VAMP7 in B16 melanoma cells. J. Biol. Chem. *276*, 19820–19827.

Wang, S., Bartido, S., Yang, G., Qin, J., Moroi, Y., Panageas, K. S., Lewis, J. J., and Houghton, A. N. (1999). A role for a melanosome transport signal in accessing the MHC class II presentation pathway and in eliciting CD4+ T cell responses. J. Immunol. *163*, 5820–5826.

Yamamoto, H., Takeuchi, S., Kudo, T., Makino, K., Nakata, A., Shinoda, T., and Takeuchi, T. (1987). Cloning and sequencing of mouse tyrosinase cDNA. Jpn. J. Genet. *62*, 271–274.

Yamamoto, H., and Takeuchi, T. (1981). Immunoelectron microscopic localization of tyrosinase in the mouse melanocyte. J. Histochem. Cytochem. *29*, 953–958.

Zhao, H., Boissy, Y. L., Abdel-Malek, Z., King, R. A., Nordlund, J. J., and Boissy, R. E. (1994). On the analysis of the pathophysiology of Chediak-Higashi syndrome. Defects expressed by cultured melanocytes. Lab. Invest. *71*, 25–34.

Zizioli, D., Meyer, C., Guhde, G., Saftig, P., von Figura, K., and Schu, P. (1999). Early embryonic death of mice deficient in γ-adaptin. J. Biol. Chem. *274*, 5385–5390.